Petroleum Science 18 (2021) 1163–1181

Contents lists available at ScienceDirect

Petroleum Science

journal homepage: www.keaipublishing.com/en/journals/petroleum-science

Original Paper

Application of sustainable basil seed as an eco-friendly multifunctional additive for water-based drilling fluids

Xin Gao [a, b], Han-Yi Zhong [a, b, *], Xian-Bin Zhang [c], An-Liang Chen [c], Zheng-Song Qiu [a, b], Wei-An Huang [a, b]

[a] Key Laboratory of Unconventional Oil & Gas Development (China University of Petroleum (East China)), Ministry of Education, Qingdao, 266580, Shandong, China
[b] School of Petroleum Engineering, China University of Petroleum (East China), Qingdao, 266580, Shandong, China
[c] Drilling Fluid Technology Services of CNPC BoHai Drilling Engineering Company Limited, Dagang, 300280, Tianjin, China

ARTICLE INFO

Article history:
Received 9 August 2020
Accepted 6 January 2021
Available online 24 May 2021

Edited by Yan-Hua Sun

Keywords:
Basil seed
Water absorbency
Multifunction
Water-based drilling fluid
Three-dimensional network

ABSTRACT

Basil seed, containing anionic heteropolysaccharides in its outer pericarp, swells as gelatinous hydrocolloid when soaked in water. In this study, basil seed powder (BSP) was used as a multifunctional additive for water-based drilling fluids. The chemical composition, water absorbency, rheological properties of aqueous suspension of BSP were tested. The effect of BSP on the rheological and filtration of bentonite-based drilling fluid before and after thermal aging was investigated. The inhibition characteristics were evaluated by linear swelling, shale cuttings dispersion and shale immersion test. Lubricity improvement by BSP was measured with extreme pressure lubricity test. The results revealed that incorporation of BSP into bentonite suspension improved rheological and filtration properties effectively after thermal aging of 120 °C. BSP exhibited superior inhibitive capacity to xanthan and synergistic effect with KCl. BSP could reduce friction by forming hydration layer. The nanoscale three-dimensional network structures enable BSP to maintain high water retention and absorb strongly on bentonite and metal surface, contributing to enhanced rheology, filtration, inhibition and lubrication properties. The versatile characteristic of BSP, as well as biodegradation makes it a promising additive using in high performance water-based drilling fluid and a potential alternative to conventional synthetic polymers.

1. Introduction

In oil and gas drilling engineering, drilling fluid is one of the most important components of drilling operations which plays the role of suspending and transporting drill cuttings, cooling the bit, maintaining wellbore stability, providing essential lubrication, and cleaning the hole (Johannes, 2012; Li et al., 2015a, b; Gudarzifar et al., 2020). The importance of properly designed muds with high functionality in the drilling process can closely resemble the function of blood in human body vessels (Ghaderi et al., 2020). In some circumstances, the success of a drilling operation primarily depends on the composition and performance of drilling fluid used, therefore, the drilling fluid additives should be carefully selected to fulfill the requirements (Al-Hameedi et al., 2019a).

With the increasing number of drilling scenarios involved in deep reservoirs, unconventional resources, complex well geometries as well as more stringent environmental regulations, high performance water-based drilling fluids with rational rheological properties, effective filtration control, high shale stabilization and lubrication are required (Tehrani et al., 2007). More importantly, the concerns about environmental protection from the detrimental effect of chemical and non-biodegradable materials increase dramatically around the world during the past decades (Al-Hameedi et al., 2019a), which motivates the researchers to develop innovative additives and drilling fluid formulations with higher safety and environmental acceptability (Li et al., 2016a, b; Ghaleh et al., 2020). During the past years, various types of additives including natural and synthetic materials have been employed. Although displaying several advantages such as higher temperature stability and better salt contamination tolerance, the

* Corresponding author. Key Laboratory of Unconventional Oil & Gas Development (China University of Petroleum (East China)), Ministry of Education, Qingdao, 266580, Shandong, China.
E-mail addresses: zhonghanyi@126.com, zhonghanyi@upc.edu.cn (H.-Y. Zhong).

https://doi.org/10.1016/j.petsci.2021.05.005

Abbreviations

AHR	After hot rolling
AOAC	Association of Official Analytical Chemists
API	American Petroleum Institute
AV	Apparent viscosity
BHR	Before hot rolling
BOD_5	5 days biological oxygen demand
BSG	Basil seed gum
BSP	Basil seed powder
CMC	Carboxylmethyl cellulose
CMS	Carboxylmethyl starch
COD	Chemical oxygen demand
EC_{50}	Concentration for 50% of maximal effect (EC_{50})
HEC	Hydroxyethyl cellulose
HPS	Hydroxypropyl starch
HTHP	High temperature and high pressure
LTLP	Low temperature and low pressure
Na-bent	Sodium bentonite
PAC	Polyanionic cellulose
PHPA	Partially hydrolyzed polyacrylamide
PV	Plastic viscosity
SEM	Scanning electron microscope
3D	Three dimensional
XC	Xanthan gum
YP	Yield point

main drawbacks associated with the high cost, non-biodegradability and negative environmental effect of synthetic additives, especially synthetic polymers, limit their wide use. Therefore, there is still a great need for new environmentally friendly acceptable and multifunctional additives that can be in favor of improving the drilling fluid properties with the least effect on the environment (Nicora and McGregor, 1998; Al-Hameedi et al., 2019a; Li et al., 2016b, d).

In recent years, many research works have been conducted on the employment of natural, biodegradable, non-toxic, and eco-friendly green materials in drilling fluids to impart a specific function or several functions. Some naturally occurring materials are used in drilling fluids directly without modification (Ghaleh et al., 2020; Kumar et al., 2020). While, more natural materials are used by chemical modification to better meet the requirements of water-based drilling fluids (Li et al., 2018; Hall et al., 2017). Among these materials, the biopolymers and their chemically modified derivatives, with primary components of polysaccharides, owing to appropriate properties, widespread availability, relatively low cost, and inherent biodegradability, are frequently used to improve drilling fluid properties such as rheological properties and filtration control (Akbari and Ghoreishi, 2017). Typically, xanthan gum, scleroglucan, guar gum, diutan and welan gum are used as viscosifiers due to their shear-thinning and thixotropic behavior (Sarber et al., 2010; Villada et al., 2017). Starch derivatives like carboxylmethyl starch (CMS) and hydroxypropyl starch (HPS), cellulose derivatives like carboxylmethyl cellulose (CMC), hydroxyethyl cellulose (HEC), and polyanionic cellulose (PAC), modified tannins and lignins are classic products that have been widely used for rheological modification and filtration control (Kafashi et al., 2017). A variety of other natural materials and their modifications have been investigated as potential drilling fluid additives. Examples include soy protein isolate (Li et al., 2015a), nanocellulose (Li et al., 2018; Zhang et al., 2018), psyllium husk (Salmachi et al., 2016), rice husk (Okon et al., 2020), grass (Hossain and Wajheeuddin, 2016), solanum tuberosum formulater biopolymer (Tomiwa et al., 2019), henna extract (Moslemizadeh et al., 2015) and carrageenans (De Oliveira et al., 2020). Some wastes such as pistachio shell powder (Davoodi et al., 2018), mandarin peels powder (Al-Hameedi et al., 2019a), potato peels powder (Al-Hameedi et al., 2019b) are also introduced in drilling fluids to function as required purpose.

Ocimum basilicum L. also known as basil is a common herb plant found in many parts of the world, especially in the tropical regions of Asia, Africa and Central and South America. Basil seeds have been used in traditional medicine since ancient times. Basil seeds are black in color and oval in shape (Akbari and Ghoreishi, 2017). Due to the presence of a polysaccharide layer, when soaking in water, the outer pericarp swells into a gelatinous mass which is called as basil seed gum (BSG). BSG is an anionic heteropolysaccharide, which consists of glucose, galacturonic acid, glucomannan, mannose, glucuronic acid, arabinose, rhamnose, and galactose (Farahmandfar and Naji-Tabasi, 2020). The two major chemical components of BSG are glucomannan (43%) and (1 → 4)-linked xylan (24.29%) (Naji-Tabasi et al., 2016) (Fig. 1). Because of the advantages of its shear-thinning behavior and good gelling properties, BSG offers potential application in various areas including remover of heavy metals, disintegrant, pharmaceutical excipient, suspending agent, anti-diabetic agent and biodegradable edible film (Naji-Tabasi et al., 2016; Mirabolhassani et al., 2016).

Basil seeds have a certain content of gum (generally ranging from 10% to 20% depending on the treating methods) with outstanding functional properties which is comparable with some other commercial gums such as xanthan (Naji-Tabasi et al., 2016; Naji-Tabasi and Razavi, 2017; Rafe and Razavi, 2013; Zameni et al., 2015). Therefore, the aim of this study is to investigate the feasibility of basil seed powder (BSP) as a potential biodegradable additives in water-based drilling fluids. Firstly, the component and structure of the BSP was characterized. Subsequently, the rheological adjustment, filtration loss control, shale inhibition and lubrication properties of the BSP-beneficiated water based drilling fluid are examined and considered. The underlying mechanism was elucidated with related characterizing methods. To the best of our knowledge, no research work has concerned about the effect of BSP on the drilling fluid properties systematically until now, which highlights our research.

2. Materials and methods

2.1. Materials

The raw basil seeds were bought from Bozhou rose fragrance Biotechnology Co., Ltd, China. Sodium bentonite (Na-bent) was provided by Weifang Huawei bentonite Group Co., Ltd, China, following the API standard. Sodium carbonate, sodium chloride, calcium chloride and anhydrous ethanol in analytical grade were purchased from Sinopharm Chemical Reagent Co., Ltd, China. All the experimental reagents were used without further purification.

Pretreatment of basil seed is required before use. The basil seeds were pulverized with a crusher by pulverizing 1 min at a stirring rate of 27000 rpm and pausing 1 min. After treated for 10 min, the pulverized powder was washed with anhydrous ethanol for several times until the filtrate became colorless. The filtered powder was dried at 80 °C for 4 h (Fig. 2). This procedure was repeated until the final BSPs could be sieved through 40 mesh.

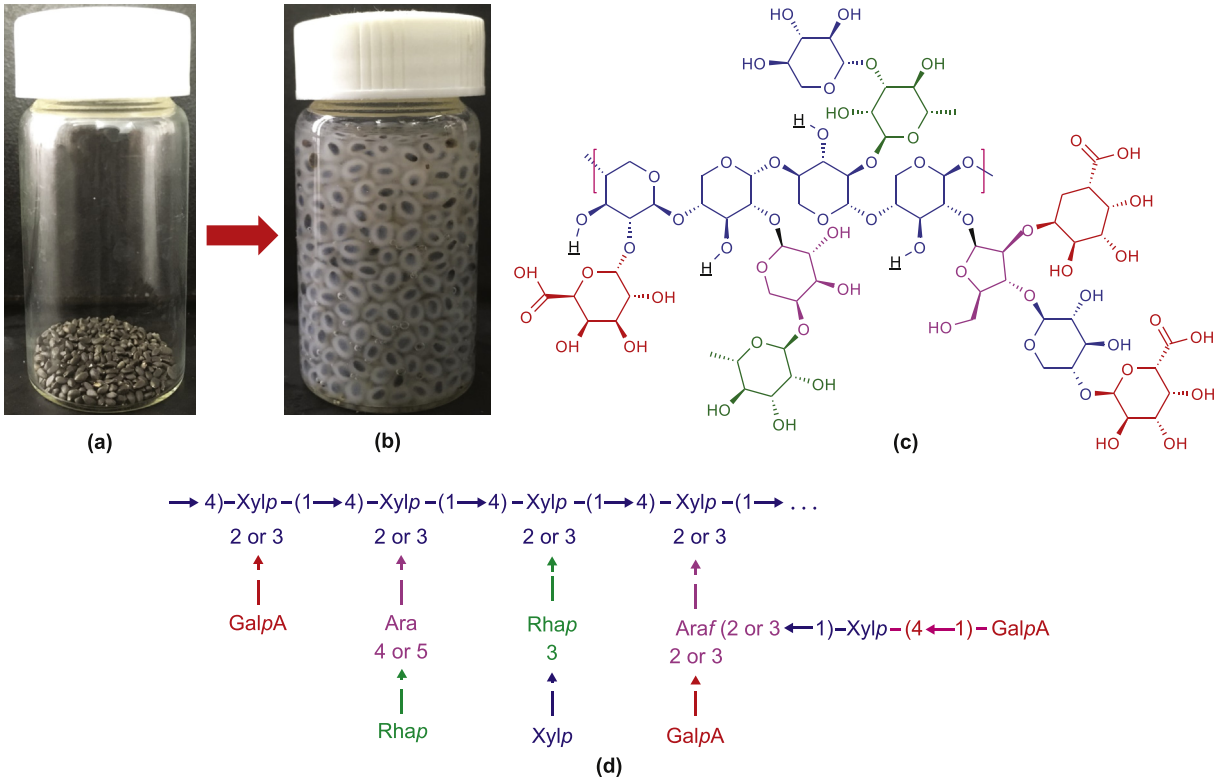

Fig. 1. (**a**) Basil seed; (**b**) basil seed after water adsorption; (**c**) chemical structure of basil seed gum; (**d**) basil repeating oligomer.

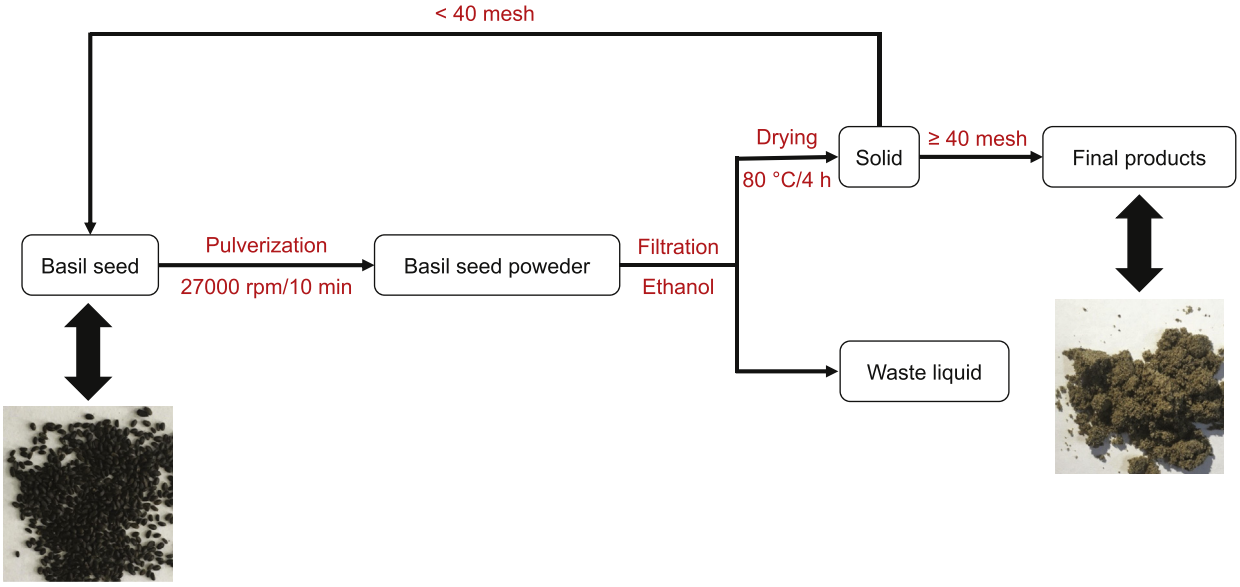

Fig. 2. The pretreatment procedure of BSP.

2.2. Characterization of basil seeds

Accurately weighed BSPs (1.00 g) were sealed in a non-woven bag and soaked in deionized water at 20 °C and 90 °C where the temperature was controlled by water bath. Once the BSPs contacting with deionized water, the variation of bag weight was weighed and recorded after specific time intervals. Before weighing, the bag was carefully taken out from water and drained the excessive water for 3 min. The swelling capacity was determined with the following equation (Lodhi et al., 2019).

$$S = \frac{m_t}{m_0} \times 100\% \quad (1)$$

where S is the swelling rate; m_t is the weight of BSP after a certain time, g; m_0 is the initial weight of BSP, g.

The moisture, oil content, protein and ash were determined according to Association of Official Analytical Chemists standard (AOAC) 930.15 and AOAC 925.10, AOAC 991.36, AOAC 968.06 and AOAC 942.05, respectively as previously described (Hosseini-Parvar

et al., 2010). The content of carbohydrate was calculated by the subtraction method.

2.3. Toxicity and biodegradability evaluation

The toxicity was measured with the luminescent bacteria method according to the National Standards of the People's Republic of China GB/T 15441-1995 (Water quality-determination of the acute toxicity-luminescent bacteria test). The concentration for 50% of maximal effect (EC_{50}) was used as the standard to determine the toxicity level. The biodegradability of BSP was determined by measuring the ratio of 5 days biological oxygen demand (BOD_5) to chemical oxygen demand (CODcr), which were estimated following the standard protocols of American Public Health Association method (Kuppusamy et al., 2017). The ratio of BOD_5 to COD_{Cr} represents the ratio of biodegradable organic matter to total organic matter (Dhanke and Wagh, 2020; Otieno et al., 2019).

2.4. Characterization of rheological properties

The bentonite-based drilling fluids (base muds) were prepared by dispersing 16.0 g of bentonite and 0.8 g of sodium carbonate in 400 mL fresh water under high shear conditions. Then the suspension was sealed and hydrated for 24 h to achieve a complete hydration. The BSPs with increasing concentrations were added to the bentonite suspension by homogenizing on a mixer for 20 min with a stirring speed of 8000 rpm. In order to simulate the environment encountered in high temperature wells, the mixed suspension was put in a sealed stainless cell and hot rolled in an oven at a setting temperature for 16 h. The exposure to this thermal aging process can also be used to judge the thermal stability of the fluids (Li et al., 2016c). For both before hot rolling (BHR) and after hot rolling (AHR), the rheological properties of the suspension were determined by an Anton Paar MCR 301 rheometer (Anton Paar, Austria) and a ZNN-D6 six-speed rotating viscometer (Qingdao Haitongda Special Instrument Co., Ltd., China), respectively. The rheology measurements were completed by the Anton Paar MCR 301 rheometer with a coaxial cylinder system. The steady state flow rheology including shear stress and viscosity was determined using a shear rate ramp from 0.1 to 1000 s^{-1} at 25 °C.

The rheological properties of the suspension were obtained by fitting experimental data into the Bingham plastic model and the Power law model. The Bingham plastic model is widely used to represent the pseudo plastic behavior of the drilling mud. The rheological parameters including plastic viscosity and yield point are obtained by fitting experimental data into Bingham model (Li et al. 2016c, 2019; Salmachi et al., 2016; Ahmad et al., 2017). The Bingham plastic model is represented by Eq. (2):

$$\tau = \tau_0 + \eta_p \gamma \tag{2}$$

where τ, τ_0, η_p and γ are the measured shear stress (Pa), yield stress (Pa), plastic viscosity (Pa s) and shear rate (s^{-1}), respectively.

The power law model is another rheological model that uses flow index (n) and consistency index (K) (Pa s^n) to describe the exponential relationship between the shear rate and shear stress of fluids. The model can be mathematically expressed as follows.

$$\tau = K\gamma^n \tag{3}$$

A model ZNN-D6 six-speed rotating viscometer was used to measure the rheological parameters including apparent viscosity (AV), plastic viscosity (PV) and yield point (YP) of the drilling fluid (Zhong et al., 2019).

2.5. Measurement of filtration properties

The low temperature and low pressure (LTLP) filtration experiments were performed with a ZNZ-D3-type medium-pressure filtration apparatus (Qingdao Haitongda Special Instrument Co., Ltd., China). The filtrate volume was collected at a differential pressure of 0.7 MPa and room temperature on filter paper for a 30-min period as recommended by the API standard (Barry et al., 2015). The HTHP static filtration loss test is designed to simulate the filtration properties similar to that of downhole conditions. After thermal aging at a certain temperature, the HTHP static filtration loss of the drilling fluid was conducted by a HTHP filter press (GGS71-B, Qingdao Haitongda Special Instruments Co., Ltd., China) with standard filter paper and controlled pressure sources of nitrogen. This test was conducted at a certain temperature equal to that of thermal aging temperature and 3.5 MPa pressure difference for a period of 30 min (Luo et al., 2018). The filtrate volume was collected and recorded by a graduated cylinder.

To investigate microscopic structure of filter cake, after the filtration test, the fresh filter cakes were firstly shock-frozen in liquid nitrogen and followed by freeze drying at −50 °C, with the purpose to remove the free water in the filter cake and the water adhering to the hydrated bentonite and avoid the change of the filter cake morphology by sublimation (Plank and Gossen, 1991). The dried samples were sputter coated with gold and analyzed by a scanning electron microscope (SEM, Sigma300, Zeiss) to evidence the micro- and nanostructures.

2.6. Measurement of shale inhibitive properties

2.6.1. Linear swelling test

The linear swelling test was devised to estimate the swelling increment of the shale after exposing to the testing fluid, and to measure the reactivity of the shale to the fluid (Li et al. 2016c, 2019). Firstly 10 g of sodium bentonite was pressed into a pellet with a diameter of 25.4 mm under the pressure of 10 MPa for 5 min. Then the pellet was put in a shale chamber of the linear swelling tester that limits the sample swelling to the vertical direction. Once the testing fluid was slowly poured into the chamber and contacted with the pellet, the displacement of the pellet due to swelling after adsorption of water was recorded with time. The swelling rate of shale pellet was calculated by the ratio of the expansion height to the original height of the pellet.

2.6.2. Shale cuttings hot-rolling dispersion test

The shale cuttings hot-rolling dispersion test was performed to evaluate the tendency of the shale sample to disintegrate after interaction with formulated fluid in a rolling oven cell at setting temperatures. A total of 50 g shale cuttings (2–5 mm) coming from the upper layer of Shahejie Formation in Shengli Oilfield of China and 350 mL testing fluid were kept in a sealed cell and hot rolled at 77 °C for 16 h. After hot rolling, the remaining shale cuttings were washed with fresh water, screened through a 40-mesh sieve, dried at 105 °C for 4 h and recovered. The shale cuttings recovery was determined by the ratio of recovered shale cuttings weight to the original shale cuttings weight.

2.6.3. Sodium bentonite immersion test

Active shale generally contains clay minerals like montmorillonite, kaolinite and illite. The hydration and dispersion of shale mainly arises from the hydration of clay minerals. Since the primary component of sodium bentonite is also sodium montmorillonite, sodium bentonite immersion test was used to evaluate the inhibitive properties of various inhibitors, which can mimic the interaction between shale and additives to a certain extent. A total of 100 g

sodium bentonite was mixed with 15 g deionized water. The mixture was pressed under the pressure of 15 MPa for 20 min to form a core with a diameter of 48.5 mm and a thickness of 14.7 mm. Then the bentonite core was soaked in the BSP suspension, and the variation of the core appearance with time was recorded and photographed. After the test, the control sample and core soaked in 1.0 w/v% BSPs were shock-frozen in liquid nitrogen and followed by freeze drying at −50 °C. After that they were examined by SEM.

2.7. Lubrication performance measurement

In order to study the effect of BSPs on improving lubricity and extreme pressure properties of the drilling fluid, the BSPs with varying concentrations were added into the bentonite-based drilling fluid and the lubricity properties was evaluated with the extreme pressure and lubricity tester. The exerted torque was 150 psi and the testing time lasted for 30 min. The reduction percentage of lubricity coefficient is calculated as follows (Dong et al., 2015; Li et al., 2016d).

$$R_L = \frac{\mu_{Bent} - \mu_{BSP}}{\mu_{Bent}} \quad (7)$$

where R_L is the reduction percentage of lubricity coefficient; μ_{Bent} is the lubricity coefficient of base mud; μ_{BSP} is the lubricity coefficient of base mud with BSPs.

3. Results and discussion

3.1. Chemical composition of basil seed

3.1.1. Fraction of basil seed

The chemical composition of the basil seeds in this study is presented in Table 1. It could be seen that carbohydrate and oil are the most abundant ingredients. The carbohydrate is the primary component for generating hydrocolloid, which imparts influence on rheological and filtration properties of drilling fluids. The oil in the basil seed shows potential as lubricant for drilling fluids. The protein contains both amine groups and carboxyl groups, therefore, it easily interacts with bentonite particles and other additives with adsorption.

3.1.2. Water absorbency

The water adsorption as a function of time is shown in Fig. 3. After soaking in water, the basil seeds adsorbed water speedily at the initial 30 min, followed by slow increment of water adsorption amount. When the testing temperature increased from 20 to 90 °C, the water absorbency increased correspondingly due to the faster spreading of water molecules under higher temperature. After soaking in water for 24 h, the water absorbency was 7.10 and 7.28 g/g at 20 and 90 °C, respectively. Meanwhile, as shown in Fig. 3, the basil seed was surrounded with a hydration layer after water absorption, making the seed smooth and elastic. The high water absorbency for basil seed indicated addition of basil seed can decrease the free water content in the drilling fluid, which is beneficial for filtration control and wellbore stability in drilling.

Table 1
The chemical composition of basil seed.

Component	Content, %
Water	7.93
Oil	22.47
Ash	3.86
Protein	19.26
Carbohydrate	46.48

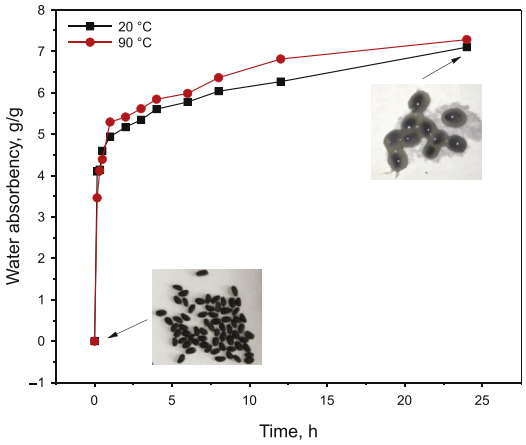

Fig. 3. Water absorbency of basil seed at room temperature and 90 °C.

3.1.3. Rheological properties of basil seed powder dispersion

Flow curves of viscosity vs. shear rate were performed for the BSP aqueous suspensions. As shown in Fig. 4a, an interesting pseudo-plastic and shear thinning behavior was observed that the viscosity decreases rapidly at shear rate from 0.1 to 1 s^{-1}, and then varies slightly at shear rate from 1 to 1000 s^{-1} across all BSP concentrations. The high viscosity at low shear rates indicated that high levels of hydration and entanglement of polysaccharide molecules formed after dispersing in water. As the shear rate increased, the aggregates were destroyed. The molecules orient along the flow direction, and the apparent viscosity decreases (Vargas et al., 2019). This high shear thinning behavior of the suspension favors for the pumping and drilling solids carrying in drilling, which is virtually desirable for drilling fluid applications (Hall et al., 2018).

The variation of shear stress with shear rate for BSP suspension suggested that power law model could be used to describe the rheological properties (Fig. 4b). The rheological parameters obtained using the power law model for BSP suspension at various concentrations are presented in Table 2. All samples exhibited a good fit to the power law model, with coefficient of determination (R^2) close to or greater than 0.95. Generally, the flow behavior index (n) decreased with an increase in the BSP concentration, indicating that the suspension became more shear thinning especially at low shear rates. Meanwhile, the consistency coefficient (K) generally increased with an increase in the BSP concentration, suggesting the increase in the viscosity of the suspension. This was also verified by the flowability observed from Fig. 5a, that the BSP suspension gradually lost the flow with the increase in concentration. When the shear rate was low, due to the high water absorbency, BSP produces high levels of hydration and leads to increased viscosity, which is beneficial for drill cuttings suspension and transportation. With an increase in the shear rate, since all hydrocolloids behave like weak gel, the polysaccharide polymers are quickly oriented in the direction of flow and therefore the aggregation of polymer chains decreases (Hosseini-Parvar et al., 2010; Naji-Tabasi and Razavi, 2017b). This favors the drilling because an extremely low viscosity is desirable for breaking rocks for the water jet at the bit nozzle.

3.1.4. Microstructures of basil seed gum

The images of 1.0 w/v% BSP aqueous suspension observed by the polarizing microscope are presented in Fig. 6. It could be seen from Fig. 6a, that a large amount of fluffy fiber bundles stretched from

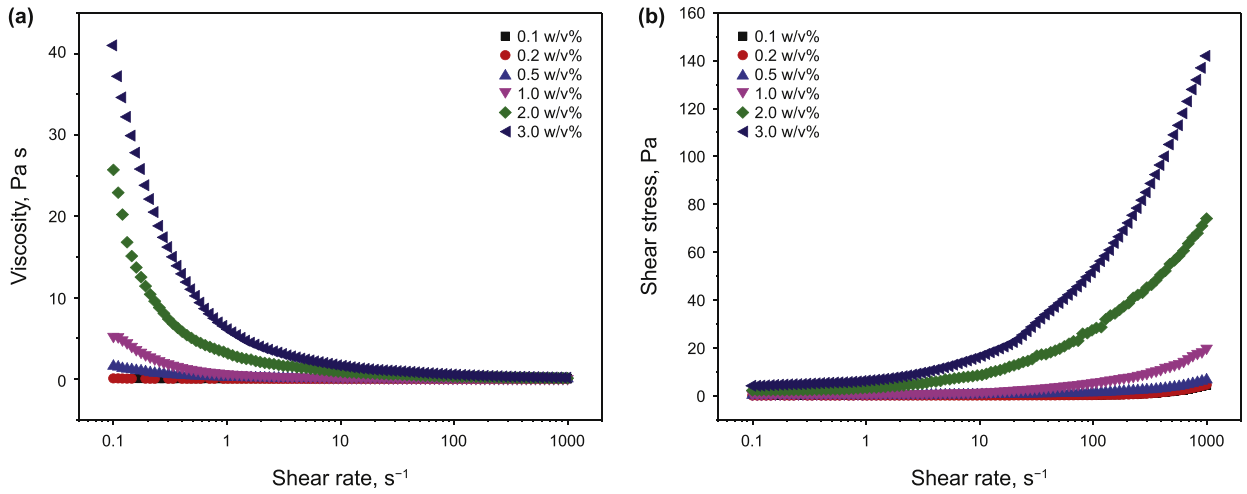

Fig. 4. Rheological properties of BSP dispersion at different concentrations.

Table 2
The rheological parameters of Power law model for BSP suspension at various concentrations.

BSP content, w/v%	K, Pa s^n	n	R^2
0.1	0.0041	0.8753	0.9543
0.2	0.0031	0.9327	0.9625
0.5	0.2299	0.3902	0.9449
1.0	0.7365	0.4202	0.9445
2.0	3.6648	0.4264	0.9857
3.0	7.1754	0.4185	0.9827

the outer pericarp of the basil seed into the aqueous solution, which provided a large space for the basil seed to imbibe water and form mucilage. These columnar structures unfolded and hold the mucilage tightly to the surface of the seed core, which was responsible for the high water imbibition and thickening effect (Nazir et al., 2017). Meanwhile part of these fiber bundles are tangled with each other to form a large aggregation structure. As shown in Fig. 6b, a considerable amount of nearly spherical particles ranging from 5 to 10 μm was also observed, attributing from the insoluble parts of the basil seeds.

The freeze-dried 3.0 w/v% BSP suspension was observed by SEM and shown in Fig. 7. As depicted in Fig. 7a, numerous tiny fibril structures are connected with each other to form a large number of flaky structures with interspaces. A magnified image presented in Fig. 7b indicated that numerous nanoscale three dimensional (3D) networks were fabricated by bundles of nano fibers and globular structures connecting with each other. Samateh et al. (2018) reported a similar structure and explained that complex branching in basil leads to this efficient 3D network and gelation capacity. These networks further converged with each other to form larger sheet structures. This highly porous structure of the basil seed gum offered an easy channel for water which is essential for fast and high swelling (Lodhi et al., 2019; Rafe et al., 2013). Meanwhile, the abundant hydroxyl groups and branched units in the polysaccharide molecule chains of basil seeds, which facilitate the formation of plenty of hydrogen bonds between the polysaccharides and water (Guo et al., 2009; Liu et al., 2014). Therefore the basil seed mucilage can hold a large amount of water as seen from Fig. 3.

3.1.5. Biodegradability and toxicity tests

As shown in Table 3, the BOD_5/COD_{Cr} of 1.0 w/v% BSP suspension is 0.5218, much higher than the standard requirement, indicating a degradable property. The ecotoxicity test result of 1.0 w/v% BSP suspension is determined to be 62000 mg/L, indicating non-toxic to the environment. Therefore, BSP is non-toxic, safe and environmentally friendly.

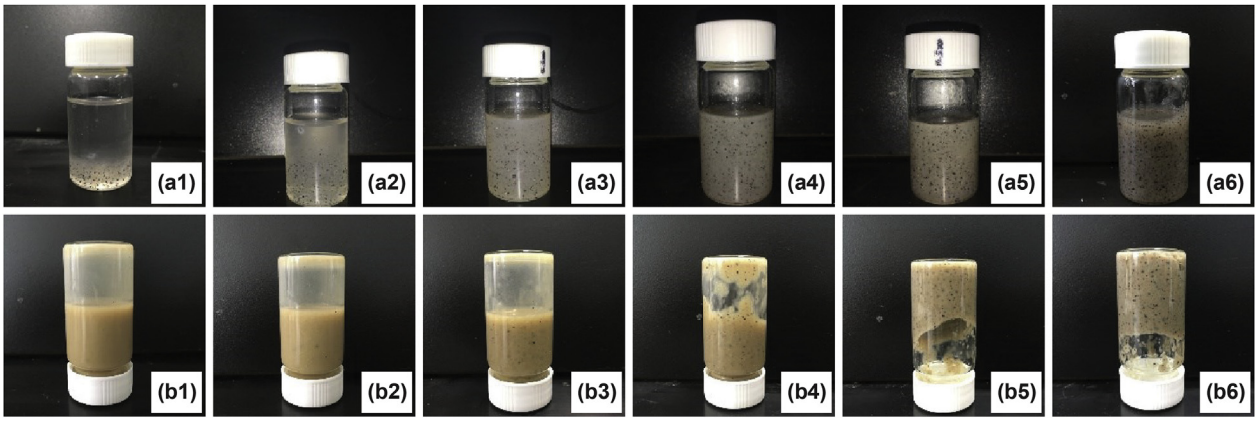

Fig. 5. Photographs of (**a**) BSP suspension and (**b**) bentonite suspension in the presence of BSP. Note: 1: 0.1 w/v%; 2: 0.2 w/v%; 3: 0.5 w/v%; 4: 1.0 w/v%; 5: 2.0 w/v%; 6: 3.0 w/v%.

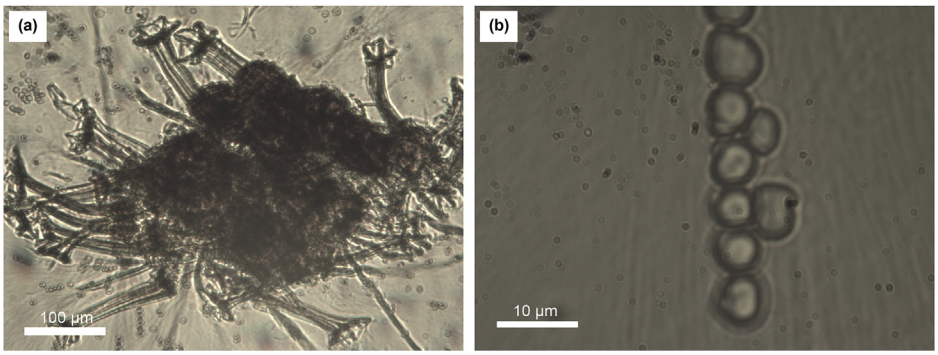

Fig. 6. The polarizing microscope photos of basil seed dispersion.

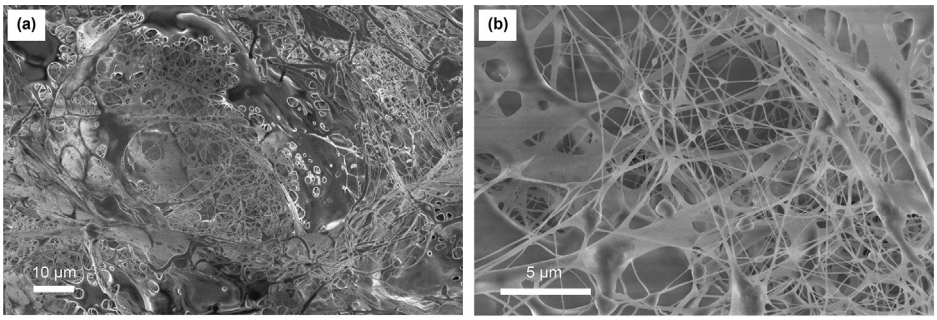

Fig. 7. SEM images of 3.0 w/v% basil seed dispersion.

3.2. Effect of basil seed on the rheological properties of bentonite suspension

Improving the rheological properties of the drilling fluid is critical for the oil well drilling operation. The effect of BSPs on the rheological properties of bentonite dispersion before and after hot rolling at 120 °C is depicted in Fig. 8. As shown in Fig. 8a and c, the viscosity decreased dramatically at low shear rates but gently at high shear rates for all the suspensions, exhibiting shear thinning behavior, which was gradually enhanced with an increase in the BSP concentration. As the BSP concentration increased, the viscosity increased correspondingly, leading to superior carrying capacity and hence better wellbore cleaning capacity. When the concentration was above 1.0 w/v%, the viscosity increased more speedily. After hot rolling, the viscosity all displayed decrement to some extent due to the degradation of basil seed gum.

Most of drilling fluids are non-Newtonian and are modelled using non-Newtonian rheological models such as Bingham plastic and power law models. The flow curves (Fig. 8b and d) were examined by fitting data to the power law model and the Bingham model respectively, and the parameters are summarized in Tables 4 and 5. The R^2 value represents the deviation between the measured experimental data and the fitted models. Regardless of thermal aging, this value obtaining from different models followed a similar trend. The R^2 values of the Bingham model were greater than that of the power law model when the BSP concentration was lower than 0.3 w/v%, and above that this trend reversed. This suggested that the suspension followed the Bingham model at low BSP concentrations but the power law model at high BSP concentrations. The reason behind this could be due to the fact that the rheological properties was dominated by the dispersed bentonite particles at low BSP concentrations. While at high BSP concentrations, the rheological properties were actually predominately controlled by the BSP. The high water absorbency and promoted gelation of bentonite particles at high BSP concentrations were probably responsible for this, which was also verified in Fig. 6b that the suspension formed a gel structure adhering to the upper part of the bottle and did not fall under the action of gravity.

In drilling operations, high viscosities are required during tripping to keep the drill cuttings suspended in the fluid at static conditions, and low viscosities are desired within the drill-string during pumping operations to clean the rock cuttings from the bottom of the well (Ogugbue et al., 2010). Therefore, the addition of BSPs into the base mud would improve the rheological properties of the drilling fluid obviously. Gel strength demonstrates the drill cuttings suspending capacity when mud pump is stopped (Salmachi et al., 2016). In the field drilling operation, the gel strength of the drilling fluid is influenced by several factors like temperature, wellbore diameter, and pumping rate. The minimum value of 10 s and 10 min gel strength should be higher than 2 and 3 Pa respectively (Ahmad et al., 2018). As shown in Table 4, the 10 s and 10 min gel strength increased gradually with the increased concentration of BSP. All the values are greater than the minimum values required, indicating enhanced drill cuttings suspending capacity.

Table 3
Biodegradability and biotoxicity test results of BSP.

Biodegradability				Biotoxicity			
BOD_5, mg/L	COD_{Cr}, mg/L	BOD_5/COD_{Cr}	Specification	Concentration, w/v%	EC_{50}, mg/L	Specification	Conclusion
1536	2943.2	0.5218	>0.3	1.0	62000	>30000 mg/L	Non-toxic

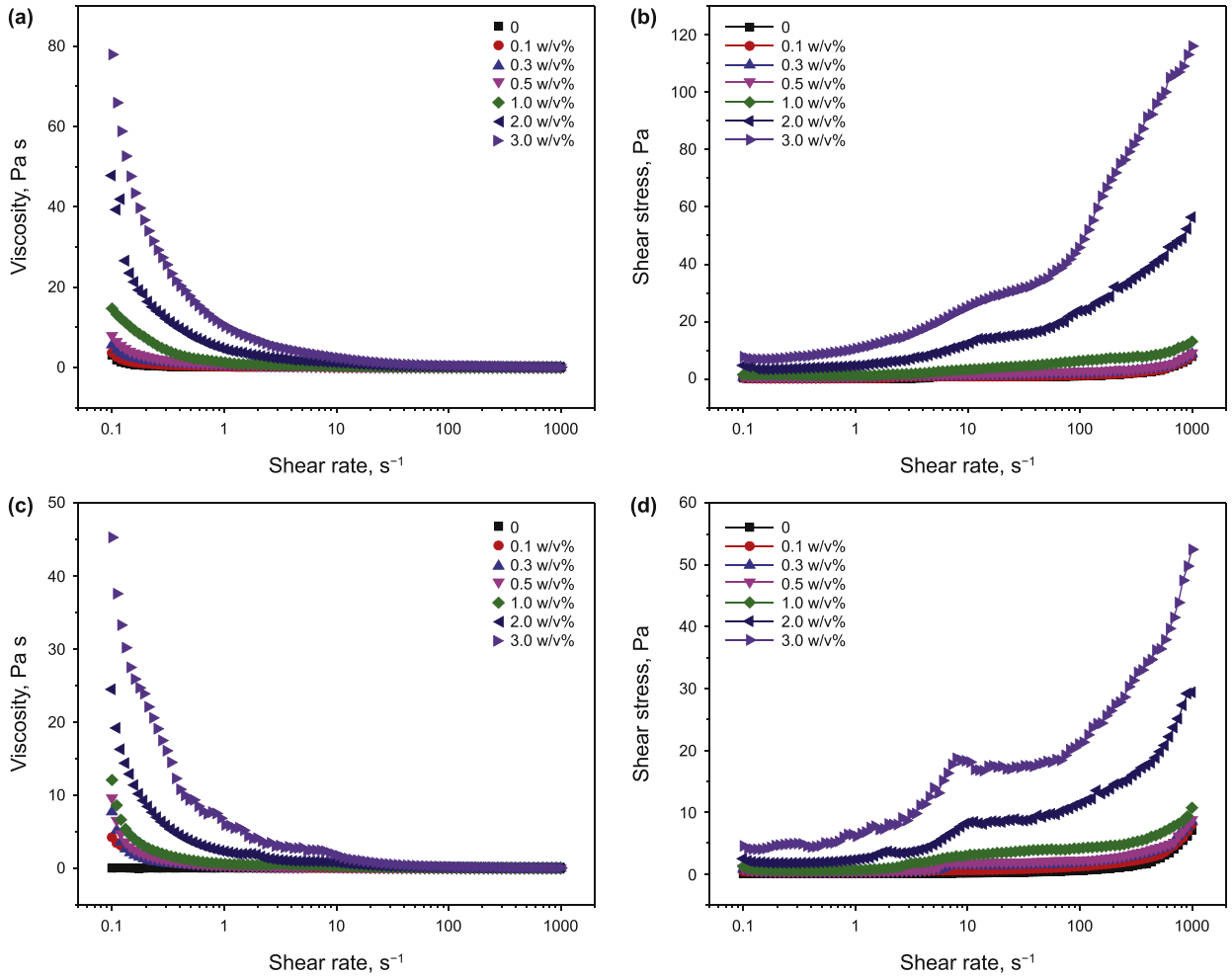

Fig. 8. Effect of BSPs on the rheological properties of bentonite dispersion before (**a, b**) and after (**c, d**) hot rolling at 120 °C.

The rheological parameters including apparent viscosityand yield point for the base mud with BSPs before and after hot rolling at various temperatures were shown in Fig. 9. Before hot rolling, the apparent viscosity and yield point increased nearly linear at the BSP concentration lower than 1.0 w/v%, but speedily at BSP concentration higher than 1.0 w/v%. An unacceptably high rheological behavior was observed when the concentration was 3.0 w/v%.

The thermal stability of the drilling fluid can be evaluated by comparing the rheological parameters before and after hot rolling at a designed temperature (Tehrani et al., 2007). It could be seen that after hot rolling at 90 and 120 °C, the rheological parameters exhibited a limited decrease, suggesting the stability of the fluid, whereas after hot rolling at 150 °C, a sharp decrease of AV and YP was observed for all the concentrations of BSPs, indicating BSP lost the ability of adjusting the rheological properties totally. The decomposition of polysaccharides by oxidation or by increased hydrolysis caused the break apart of the polymers and drop of molecular weight (Vargas et al., 2019). Thus, the BSPs could be used in high temperature environments as high as 120 °C.

3.3. Filtration control properties

3.3.1. Filtration control ability of BSP suspension

To examine the filtration control properties of BSPs, both the bentonite suspension and BSP suspension with equal concentration were prepared, then the LTLP filtration volumes were recorded and

Table 4
The rheological parameters of the power law and Bingham models for bentonite suspension in the presence of BSPs before hot rolling.

BSP content, w/v%	Gel strength, Pa		Power law model			Bingham model		
	10 s	10 min	K, Pa s^n	n	R^2	η_p, Pa s	τ_0, Pa	R^2
0	2.5	3.5	0.1723	0.4467	0.8856	0.0064	0.3019	0.959
0.1	2.5	3.5	0.3372	0.3492	0.9061	0.0065	0.4996	0.9541
0.3	2.0	4.0	0.5869	0.2911	0.9310	0.0071	0.8205	0.9520
0.5	2.0	5.0	0.8724	0.2636	0.9613	0.0073	1.2648	0.9005
1.0	3.5	7.5	1.7118	0.2667	0.9444	0.012	2.7628	0.7719
2.0	7.5	14.5	5.4987	0.3168	0.9781	0.0583	9.7365	0.8369
3.0	12.5	20.5	11.366	0.3279	0.9883	0.1331	20.502	0.8345

Table 5
The rheological parameters of the power law and Bingham models for bentonite suspension in the presence of BSPs after hot rolling.

BSP content, w/v%	Gel strength, Pa		Power law model			Bingham model		
	10 s	10 min	K, Pa s^n	n	R^2	η_p, Pa s	τ_0, Pa	R^2
0	0.5	3.0	0.0182	0.7854	0.9701	0.0060	0.0272	0.9700
0.1	1.0	3.5	0.3974	0.2800	0.8622	0.0064	0.4257	0.9774
0.3	2.0	4.0	0.3800	0.3692	0.8824	0.0072	0.6847	0.9310
0.5	2.5	4.5	0.5399	0.3328	0.8619	0.0072	0.9681	0.8785
1.0	3.5	7.0	0.9934	0.3222	0.9080	0.0092	1.9423	0.7623
2.0	6.0	11.5	2.8639	0.3154	0.9665	0.0289	5.1077	0.8425
3.0	7.0	11.5	6.9465	0.2716	0.9626	0.0487	11.303	0.8056

compared. As shown in Fig. 10a, in the case of bentonite suspension, the suspension was filtered out completely for just 3, 4, 9 and 18 min for bentonite content of 0.1, 0.2, 0.3 and 0.5 w/v% respectively, suggesting effective filter cakes were not formed. When the bentonite content was higher than 0.5 w/v%, the filtration loss tested at a duration of 30 min decreased gradually from 87.3 mL to 38.8 mL at 3.0 w/v% bentonite content. For BSP suspension, although a high filtration loss volume of 118 mL was observed at 0.1 w/v%, it performed much better than bentonite particles (Fig. 10b). The filtration loss could be reduced to as low as 18.5 mL at 3.0 w/v%, exhibiting a reduction of 52% compared to that of bentonite suspension. The above comparison results indicated that BSPs alone displayed excellent filtration control properties.

Filtration is typically controlled by both the buildup of a competent filter cake, which bridges porosity at the surface of a formation, as well as the viscosity of the fluid (Hall et al., 2018). The LTLP filtration cake of the BSP suspension was freeze dried and observed by SEM. As shown in Fig. 11a and Fig. 11b, at 1.0 w/v% BSP concentration, numerous nanoscale fibers were connected with each other to form networks. Due to the exceptional water retention ability, the movement of water molecules would be restricted, which in turn resulted in the effective filtration control. As the BSP concentration increased to 3.0 w/v%, as shown in Fig. 11c and d, more and more fibers were assembled to form a large amount of flaky structures, which potentially formed a hydration layer or a hydration film on the surface of the filter cake. Meanwhile, considerable globular microspheres were also observed, which were capable of sealing the micro pores of the filter cake. What is more, the viscosity at this concentration is much high, which reduced the filtration loss (Caenn and Chillingar, 1996; Kelessidis et al., 2013; Leerlooijer et al., 1996).

3.3.2. *Effect of BSP on the filtration properties of bentonite suspensions*

The effect of BSPs on the LTLP filtration and HTHP filtration after hot rolling at various temperatures is described in Fig. 12. In the absence of BSPs, both LTLP and HTHP filtration loss volumes increased with the hot rolling temperature, suggesting that elevated temperature gradually destroyed the hydrated structure and promoted the coagulation of bentonite particles. In the presence of BSPs, as seen from Fig. 12a, the LTLP filtration decreased speedily at the BSP concentration below 1.5 w/v% and then varied slightly after that. In comparison with the control sample, the filtration loss reduction rate was 67.1%, 64.7%, 61.3% and 40.3% for the base mud with 1.5 w/v% BSPs before and after hot rolling at 90, 120, and 150 °C, respectively. Although the thermal aging induced some degree of degradation, BSPs exhibited effective filtration control after hot rolling at 90 and 120 °C, and a less efficiency after hot rolling at 150 °C. As shown in Fig. 12b, the HTHP filtration loss decreased with increasing BSP concentration after hot rolling at 90 and 120 °C, whereas after hot rolling at 150 °C, it increased again at the BSP concentration surpassing 1.5 w/v%. Overall, the BSPs were capable of effectively controlling filtration loss at elevated temperature below 120 °C.

The morphologies of the freeze-dried filter cakes observed by SEM delivered detailed information about the structures of filter cakes. As shown in Fig. 13a, in the case of bentonite suspension before hot rolling, the clay particles oriented with edge-to-face arrangement and formed a gel structure, which restricted the movement of water. Because of some aggregation of the clay particles, a large amount of heterogeneous and irregular pores was formed, which contributed to the relatively high filtration loss volume. After the addition of 1.0 w/v% BSPs, flaky structures

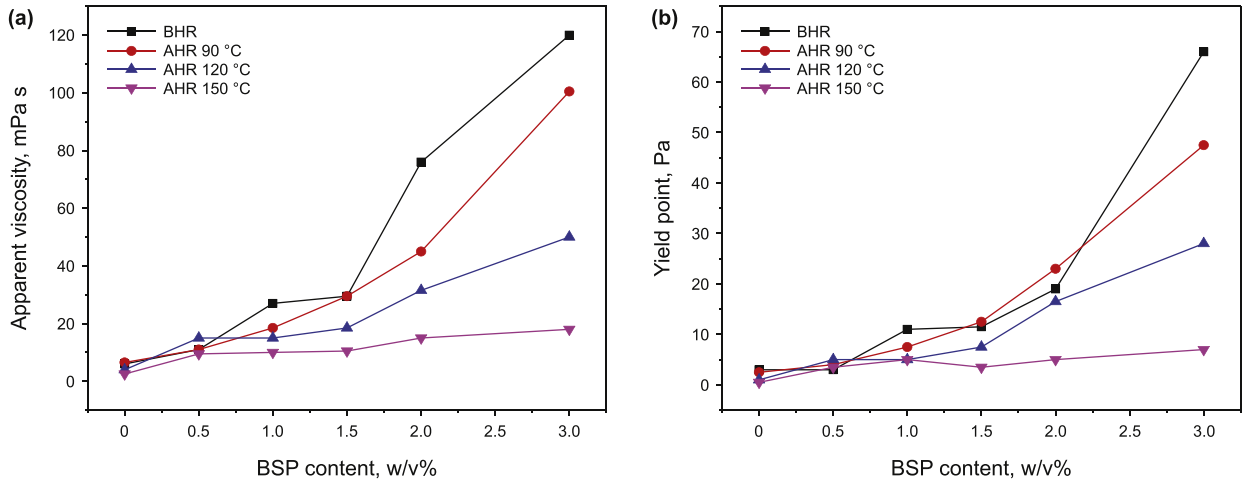

Fig. 9. Variation of rheological parameters with BSP content.

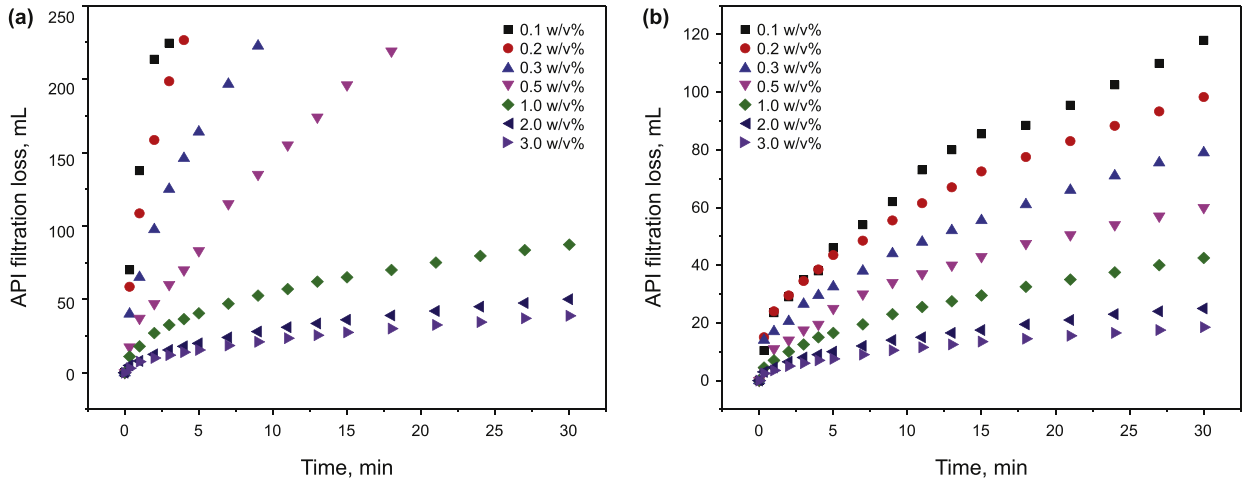

Fig. 10. LTLP filtration loss as a function of time for (**a**) bentonite suspensions and (**b**) BSP suspensions of various concentrations.

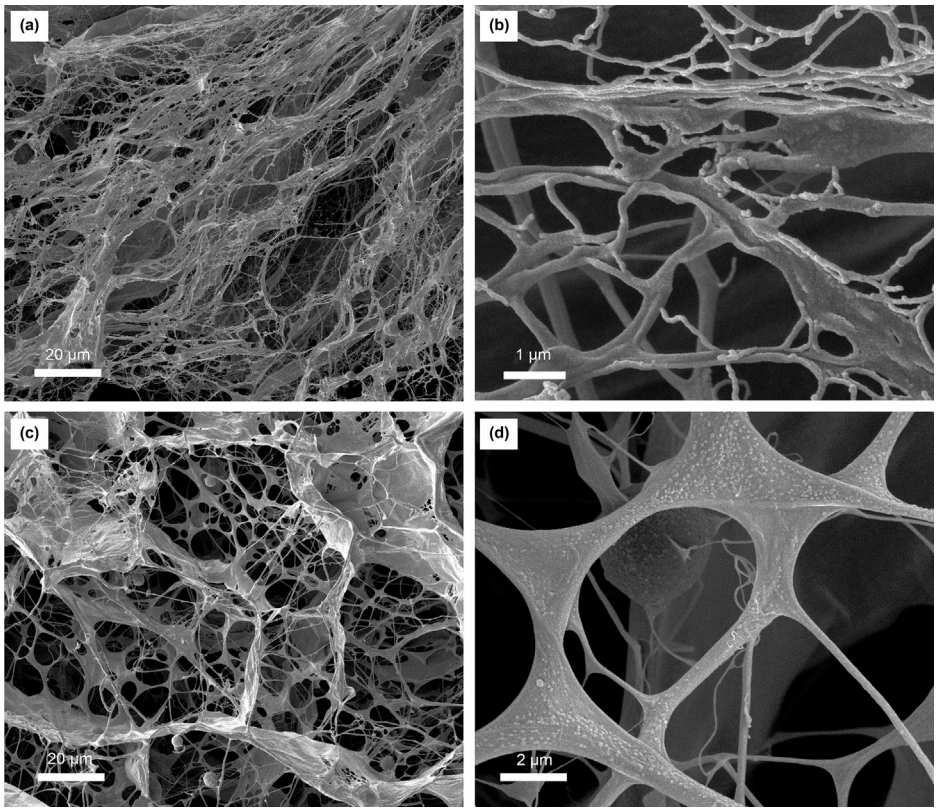

Fig. 11. SEM images of filter cakes of basil seed suspensions. (**a**) and (**b**) 1.0 w/v%; (**c**) and (**d**) 3.0 w/v%.

combined with strands were observed to form honeycomb structures, indicating typical polymer encapsulating and bridging structures, which favored the water retention and reduced the filtration loss. Meanwhile, the insoluble globular microspheres from the BSPs were also found to fill the pores of the filter cake (Fig. 13b). After exposure to thermal aging, the dehydration of clay particles occurred. The clay particles tended to form face-to-face arrangements, which provided an enlarged filtration channel and less efficient filtration control (Fig. 13c). Although some thermal degradation occurred for the polysaccharides in BSPs, as depicted in Fig. 13d, the filter cake with BSPs still exhibited a typical honeycomb structures, suggesting that BSPs were still effective in filtration control.

3.3.3. Tolerance to salt contamination

The effect of inorganic salts including NaCl and $CaCl_2$ on the rheological and filtration properties of bentonite suspension with 1.0 w/v% BSPs after thermal aging at 120 °C is presented in Table 6. For the bentonite suspension in the presence of 1.0 w/v% BSP, before thermal aging, the apparent viscosity decreased slightly with the increase in the NaCl content and then increased again. While for yield point, it increased initially with the increase in the NaCl

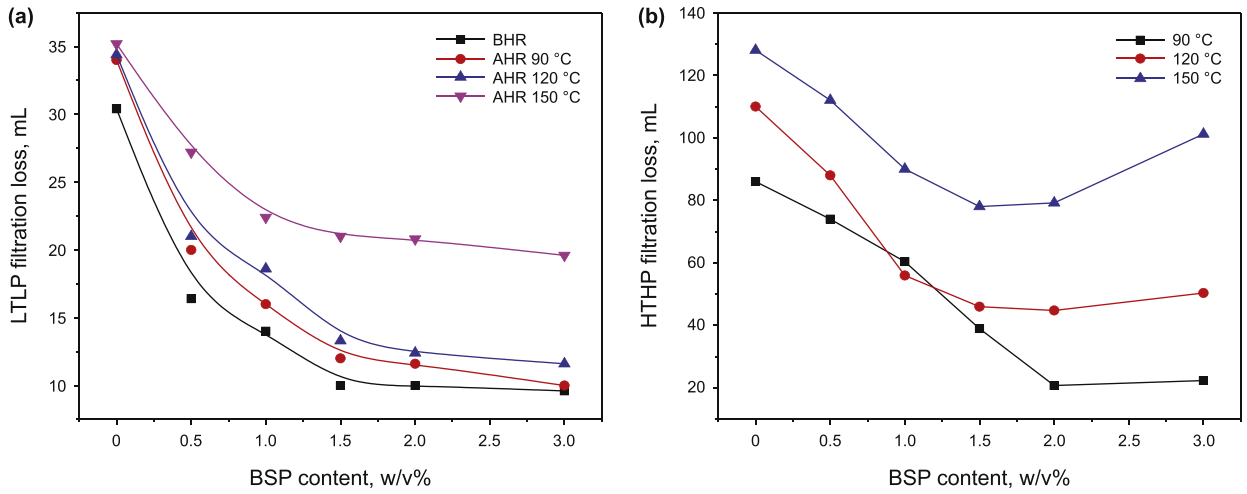

Fig. 12. Effect of BSPs on (**a**) LTLP and (**b**) HTHP filtration properties of bentonite suspensions before and after thermal aging at various temperatures.

content and then decreased. In the case of LTLP filtration loss, it increased gradually with the increase in the NaCl content. After thermal aging at 120 °C, the apparent viscosity followed a similar trend to that of before thermal aging. However, the yield point kept a continued decrease with the increasing NaCl content. When the NaCl content was above 5 w/v%, the yield point value dropped more than a half, indicating a deteriorated rheology. In terms of filtration loss, a higher filtration loss was also observed at this point. Therefore, it can be drawn that the upper limit of NaCl tolerance of the suspension is 5 w/v% by an overall consideration of rheology and filtration. From Table 6, it also could be seen that the suspension is capable of resisting 0.3 w/v% $CaCl_2$ contamination.

The addition of salt suppresses the electrical double layer of clays and results in flocculation. Meanwhile, the thermal aging further increased the probability of montmorillonite flocculating in the presence of an electrolyte (Shah et al., 1985). Due to the lattice substitution effect, the clay particles are assumed to be positive on the edges and negative on the faces. The clay particles are associated with each other with edge-to-edge, edge-to-face types and forming "card-house" structures. With the increase in temperatures, owing to the partial destruction the hydration shell, the potential of aggregation increased. When inorganic salts are added, an increase in temperature increases the ionic activity and solubility of soluble salts. The double layers are compressed by the salts and the repulsion between particles decreases, which exacerbates the aggregation of bentonite particles (Browning and Perricone, 1963; Hiller, 1963; Luckham and Rossi, 1999; Xu et al., 2020) (Fig. 14).

As shown in Fig. 15a, the incorporation of 10 w/v% NaCl and 0.5 w/v% $CaCl_2$ induced the filtration loss increased significantly from 18.6 mL to 88 and 132.5 mL, respectively, indicating the losing of filtration control. However, after the addition of 1.0 w/v% BSP, the LTLP filtration loss remarkably reduced to 30.5 mL and 58 mL,

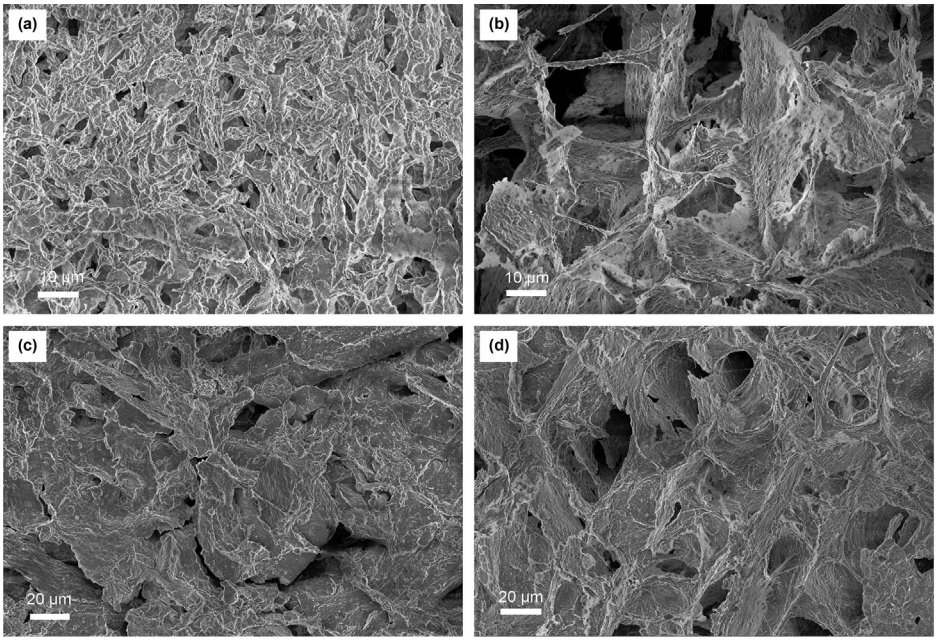

Fig. 13. SEM images of LTLP filtration cake: (**a**) bentonite suspension before thermal aging; (**b**) bentonite suspension with 0.5 w/v% BSP before thermal aging; (**c**) bentonite suspension after thermal aging; (**d**) bentonite suspension with 0.5 w/v% BSP after thermal aging.

Table 6
Effect of NaCl and $CaCl_2$ on the rheological and filtration properties of bentonite suspension in the presence of 1.0 w/v% BPS before and after thermal aging at 120 °C.

NaCl content, w/v%	Testing condition	AV, mPa s	YP, Pa	LTLP filtration, mL	$CaCl_2$ content, w/v%	Testing condition	AV, mPa s	YP, Pa	LTLP filtration, mL
0	BHR	27	11	14.0	0	BHR	27	11	14.0
	AHR	15	5	18.6		AHR	15	5	18.6
1	BHR	24	11	15.6	0.1	BHR	28.5	13	14.0
	AHR	10.75	3.75	19.2		AHR	17	5	20.8
2	BHR	26.5	15.5	18.4	0.2	BHR	31	16	18.0
	AHR	8	3	21.8		AHR	13.75	3.75	21.8
3	BHR	27	16.5	17.6	0.3	BHR	25.5	13.5	18.8
	AHR	9	3	23.2		AHR	9.5	3.5	28.8
5	BHR	28.5	14	20.8	0.5	BHR	21	11.5	22.0
	AHR	11	3	24.2		AHR	6.5	1	58.0
10	BHR	28	9.5	21.6	1.0	BHR	18	8	22.8
	AHR	10	2	30.5		AHR	6.25	0.25	80.4
15	BHR	27.5	9.5	22.0					
	AHR	9.25	2.25	31.6					

responding to a reduction rate of 65.3% and 56.2%, respectively. The thickness of the filter cake after addition of NaCl and $CaCl_2$ was 5.12 and 4.12 mm, which decreased to 1.26 and 1.54 mm, respectively, in the presence of 1.0 w/v% BSP (Fig. 15b). This suggested that BSPs could improve the salt tolerance of bentonite suspensions effectively in terms of filtration control.

Previous study indicated that the adsorption of polymer onto the surface of clay particles intrinsically does not facilitate filtration loss control. However, in saline environments the adsorption is necessary. The addition of an electrolyte reduces the electrostatic repulsion between a polyelectrolyte and clay particle, and the solvent power of water (Shah et al., 1985). The net result is higher adsorption for the anionic polysaccharides. Especially for the divalent ions of Ca^{2+}, they could function as bridges to link the anionic polysaccharides to the surface of bentonite particles. Since polyanions also have an electrical double layer, and expanded conformations in solution because of intermolecular charge repulsions. Therefore, the promoted adsorption of polysaccharide could act as good protective colloids to prevent clay particles flocculating in salt solutions (Burchill et al., 1983). This was also verified by SEM observation in Fig. 16. As shown in Fig. 16a, the bentonite particles became seriously flocculated and formed much large particles after the addition of NaCl, which resulted in large pores for filtration loss. Whereas in the presence of 1.0 w/v% BSPs (Fig. 16b), due to the adsorption between Na^{+} ions and anionic polysaccharides, a large number of cuboid NaCl crystals grew and mixed with bentonite particles to generate a relatively dense filter cake. Since divalent ions have a more profound effect on the bentonite particles, a more severe flocculation occurred after incorporation of $CaCl_2$. As shown in Fig. 16c, there were numerous pores resulting from the flocculation of bentonite particles, responding to losing control of filtration. However, the addition of BSP showed a totally different appearance. As shown in Fig. 16d, the bentonite particles still maintained small particles to form a relatively dense filter cake (Ahmad et al., 2018; Ahmed et al., 1981; Clements et al., 1987).

3.4. Shale hydration inhibitive properties

3.4.1. Linear swelling test

As shown in Fig. 17a, when contacting with deionized water at the initial time, the height of the shale pellet increased speedily, then followed by relatively slow rate. After testing for 8 h, the linear swelling rate reached as high as 37.8%. While the linear swelling rate decreased gradually with the increase in the BSP content. As the content reached 2.0 w/v%, a significant decrease was observed. The linear swelling rate was only 8.5% at 3.0 w/v% BSP, demonstrating an effective shale hydration and swelling inhibitive property. To compare the inhibitive properties, as shown in Fig. 17b, typical shale inhibitors including PHPA, KCl and low molecular weight polyamine were also employed. The linear swelling rate of the shale pellet after 8 h was 24.5%, 34.6% and 30.2% for 1.0 w/v% PHPA, 3.0 w/v% KCl and 1.0 w/v% polyamine, respectively. It could be seen that 1.0 w/v% BSP suspension exhibited a higher shale swelling rate than PHPA, but lower than polyamine and KCl. BSP exhibits comparable inhibitive property to these inhibitors.

3.4.2. Shale cuttings hot rolling dispersion test

The shale cuttings recovery of various inhibitor solutions is depicted in Fig. 18. It could be seen that 0.5 w/v% BSP suspension improved the shale cuttings recovery from 39.2% to 87.0%, demonstrating a superior performance to XC and KCl, and comparable to typical shale encapsulating agent partially hydrolyzed polyacrylamide (PHPA). Furthermore, a synergistic effect was achieved as evidenced by the fact that the combination of BSP and KCl showed the further higher shale cuttings recovery, similar to PHPA. The shale cuttings before and after hot rolling dispersion test were photographed and shown in Fig. 19. In comparison with Fig. 19a and b, the shale cuttings became smooth and round after washing the hydrated clay particles. However, as shown in Fig. 19c, the shale cuttings almost kept original shape without hydration and dispersion. What is more, a smooth film that was adsorbed on the shale cuttings was clearly observed. The extended fibers in the mucilage clung tightly to a layer of water surrounding the fiber (Samateh et al., 2018), which effectively hindered the interaction of water with shale surface and increased the resistance of shale against the rolling. The adsorbed protection layer was not observed in XC solution (Fig. 19d) and PHPA solution (Fig. 19g). When BSP and KCl were used in combination, the adsorbed film was also observed, and the shale cuttings also kept almost original shapes without hydration swelling and dispersion (Fig. 19f). Potassium ions can enter into the interlayer of the clay platelets and exchange the cations like sodium ions associated with water molecules, which reduces the hydration repulsion effectively. The high molecular polysaccharides in basil seed gum cannot penetrate into the interlayer gallery because of large molecular size, but adsorb on the surface of clay particles acting as an encapsulating coating (Guerrero and Guerrero, 2006). The hydration inhibition by potassium and encapsulation with basil seed gum in combination contributed to the effective shale hydration and dispersion inhibition. By comparison Fig. 19c and d, a conclusion could be drawn that although BSG and XC were both anionic polysaccharides, BSG demonstrated a higher and stronger adsorption capacity than XC, which could probably explain the higher shale cuttings recovery.

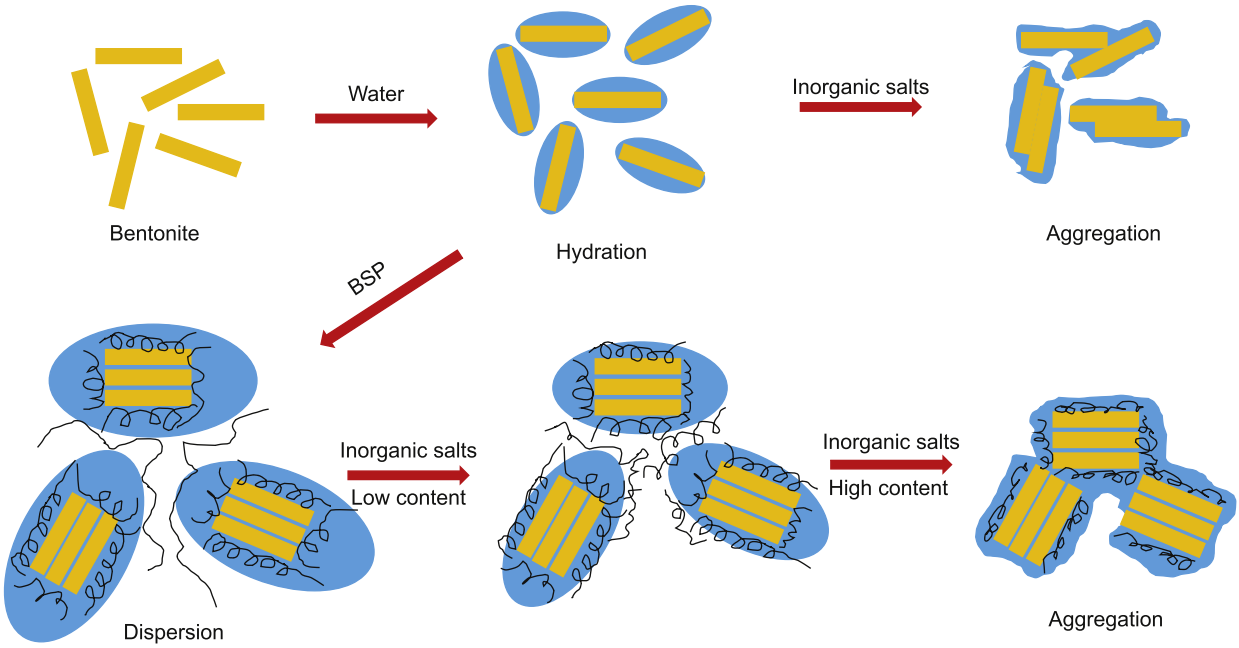

Fig. 14. The effect of inorganic salts on the associated structures of bentonite particles in the presence of BSP.

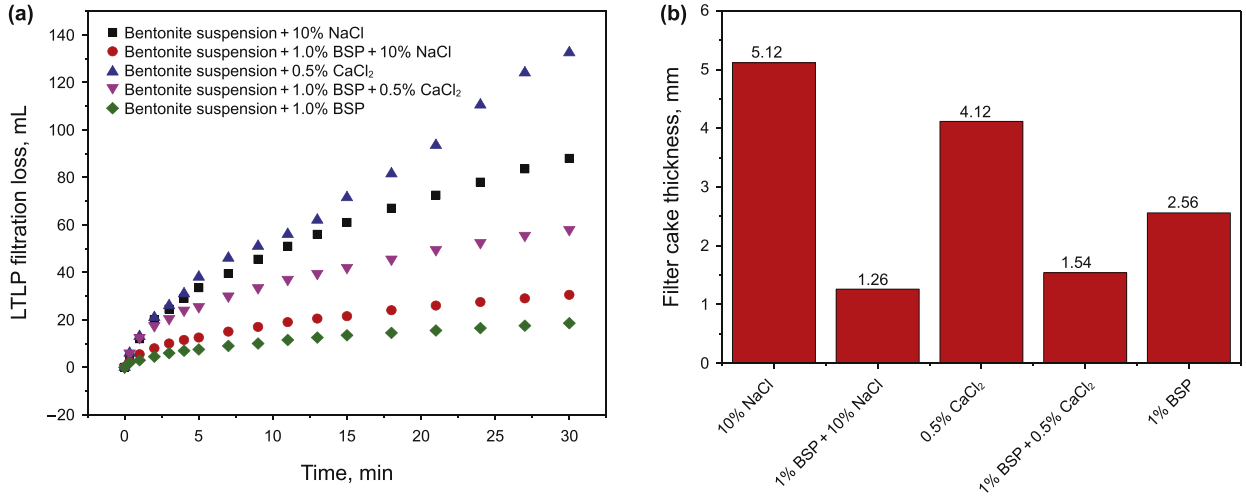

Fig. 15. Evolution of LTLP filtration with time for bentonite suspensions with 1.0 w/v% BSP under salt contamination.

3.4.3. Sodium bentonite immersion test

The variation of compressed artificial shale cores immersing in BSP suspensions with time was photographed and presented in Fig. 20. For the control sample of deionized water, it was observed that the shale core swelled and deformed obviously after immersing in deionized water for 30 min. A few tiny fractures appeared after testing for 4 h. After interaction with water for 24 h, a large number of cyclic cracks formed. The bentonite particles at the edge of the core became much loose. While in the case of BSP suspensions, different change of shale core with time was observed. As the BSP concentration increased, the swelling rate of the shale core decreased gradually. After testing for 24 h, a more integral and denser shale core was obtained. Especially for 1.0 w/v% and 3.0 w/v % BSP suspension, there were no cracks and obvious expansion appearing for the shale cores after testing for 24 h, indicating that the adsorption of BSP effectively prevented the interaction between the clay particles and water.

A small part of bentonite from the surface the shale core was freeze-dried and examined by SEM. As shown in Fig. 21a, in the absence of shale inhibitor, the clay particles hydrated thoroughly into small particles and formed house and card structures, which provided adequate space for water adsorption. There were a large amount of pores actually filled with adsorbed water before freeze drying. However, after incorporation with 1.0 w/v% BSP, the adsorption of polysaccharides onto the surface of bentonite particles via various interactions inhibited the clay hydration and dispersion (Benchabane and Bekkour, 2006). The adsorbed polymers could form a layer of film and cover the bentonite surface,

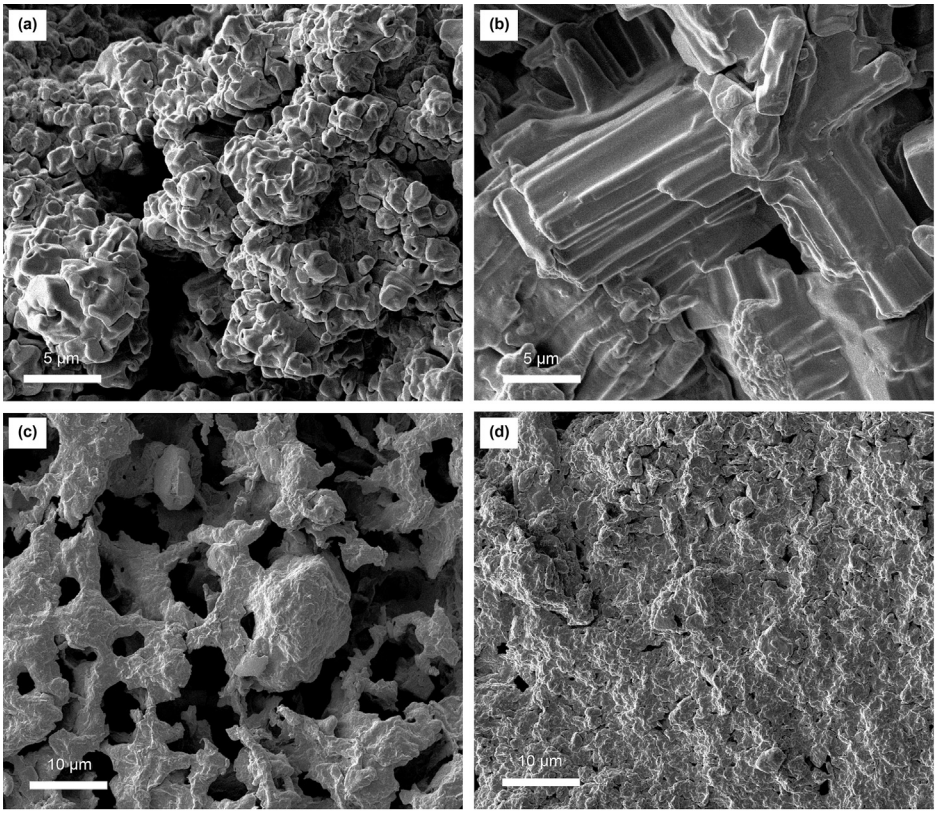

Fig. 16. SEM images of LTLP filtration cakes: (**a**) bentonite suspension with 10.0 w/v% NaCl; (**b**) bentonite suspension in the presence of basil seed polluted with 10.0 w/v% NaCl; (**c**) bentonite suspension polluted with 0.5 w/v% $CaCl_2$; (**d**) bentonite suspension in the presence of basil seed polluted with 0.5 w/v% $CaCl_2$.

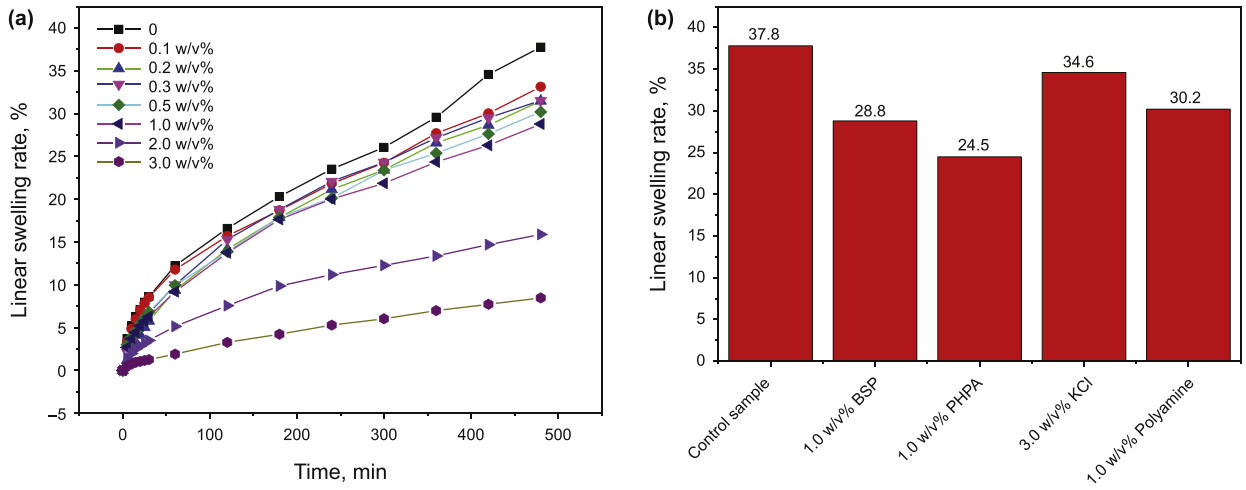

Fig. 17. Linear swelling test of (**a**) BSP dispersion with varying content and (**b**) various shale inhibitor solutions.

which hindered the ingress of water (Fig. 21b). Furthermore, the polysaccharides could stabilize the clay by thickening the liquid phase and limit the invasion rate.

3.5. Lubrication performance

After adequate water adsorption, the BSP suspension became slimy and slippery, which indicated it may have outstanding lubricating characteristic. Therefore, the variation of extreme pressure lubrication coefficient for bentonite suspension with BSPs before and after thermal aging at various temperatures was measured and shown in Fig. 22. The lubrication coefficient decreased dramatically at low concentrations of BSPs, and followed a mild change above 1.0 w/v%. In the presence of 1.0 w/v% BSP, the lubrication coefficient was reduced by 46%, 52% and 60% for the fluid before and after hot rolling at 90 and 120 °C, respectively. It seemed that thermal aging enhanced the lubricity of BSPs.

According to the characterization of BSP, the oil content is about 8.17%. There were many types of organic acids including linolenic acid, linoleic acid, oleic acid, palmitic acid, and stearic acid as well

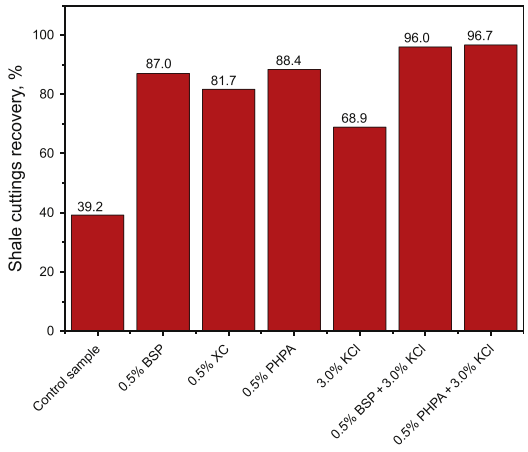

Fig. 18. Shale cuttings recovery of various inhibitor solutions.

as triacylglycerides, monoacylglycerides and diacylglycerides (Naji-Tabasi and Razavi, 2017a). These constitutes all delivered lubricity performance to some degree. What is more, a stable adsorption of basil seed mucilage on the metal surface changed the contact between metal surfaces into gel layer. Because of large amounts of hydrophilic groups in the polysaccharide molecules, such as hydroxyl group and carboxyl group, water molecules can be adsorbed on the polysaccharide network firmly by hydrogen bond to form hydrated layers (Li et al. 2012, 2016d). Those water molecules form thin hydration layers on the surface of layered sheets and are hard to be extruded out because of strong adsorption (Zhang et al., 2016). In the process of slide with friction, the mucilage of BSP is pressurized and flow away from the contact. As the contact moves across the material surface, the hydration water molecules are able to exchange rapidly with other hydration or free water molecules and are able to behave fluidly when sheared at rates lower than these exchange (relaxation) rates (Milner et al., 2018), which resulted in improved boundary lubrication. This lubrication mechanism is mainly attributed to the formation of a hydrogen-bond network between the hydrophilic groups and the water molecules (Liu et al., 2014), which differed from general lubricating behaviors.

3.6. Compatibility with typical water-based drilling fluids

To evaluate the compatibility of BSP with other drilling fluid additives, the rheological and filtration properties of two typical water-based drilling fluids (Table 7) with and without 1.0 w/v% BSP before and after thermal aging at 120 °C were measured and presented in Table 8. It could be seen that incorporation of BSP into the two drilling fluids resulted in increased apparent viscosity, plastic viscosity, yield point and gel strength. Especially for the YP/PV, which can be used to reflect the drill cuttings transportation capacity, exhibited obvious increase after thermal aging in the presence of BSPs, indicating that BSPs have positive effect on the rheological properties of the two water-based drilling fluids. In terms of filtration control, after thermal aging, the addition of BSP decreased the LTLP filtration loss by 36.7% and 38.2% for formula 1 and formula 2, respectively.

3.7. Feasibility analysis

Generally, the geothermal gradient ranges from 2 to 5 °C/100 m. Taking 3.5 °C/100 m as an average and assuming the surface temperature of 20 °C, it can be calculated that the BSP-enhanced drilling fluid with high temperature resistant of 120 °C can be used in drilling formation with a depth limit of near 3000 m. According to the above results, the excessive addition of BSP into the drilling fluid induces a sharp increase of rheological parameters, therefore, in the field application, the BSP aqueous suspension is suggested to prepare in advance and added into the drilling fluid with a low blending speed. In addition, like other biopolymers, after addition of BSP, appropriate content of bactericides are also recommended to add into the drilling fluid correspondingly to avoid fermentation.

The current results from the conducted experiments confirm that BSP behaves to be a multifunctional additive with desirable properties. Adding BSP to the drilling fluid exhibits improved

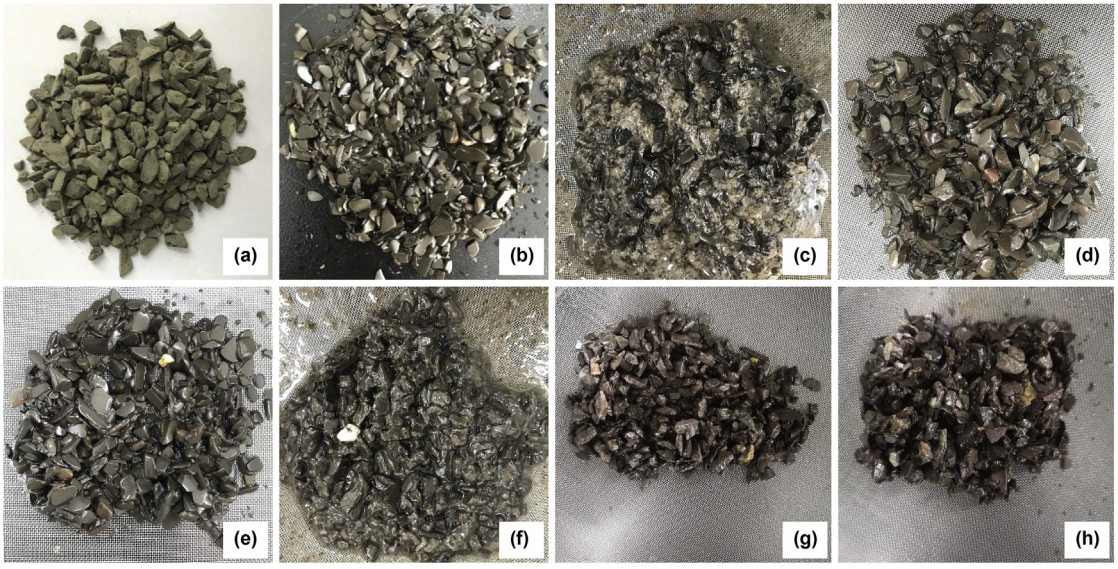

Fig. 19. Recovered shale cuttings before and after interaction with various shale inhibitors: (**a**) shale cuttings before the tests; (**b**) recovered shale cuttings after interaction with fresh water; (**c**) recovered shale cuttings after interaction with basil seed suspension; (**d**) recovered shale cuttings after interaction with XC solution; (**e**) recovered shale cuttings after interaction with KCl solution; (**f**) recovered shale cuttings after interaction with suspension having basil and KCl; (**g**) recovered shale cuttings after interaction with PHPA solution; (**h**) recovered shale cuttings after interaction with solution having PHPA and KCl.

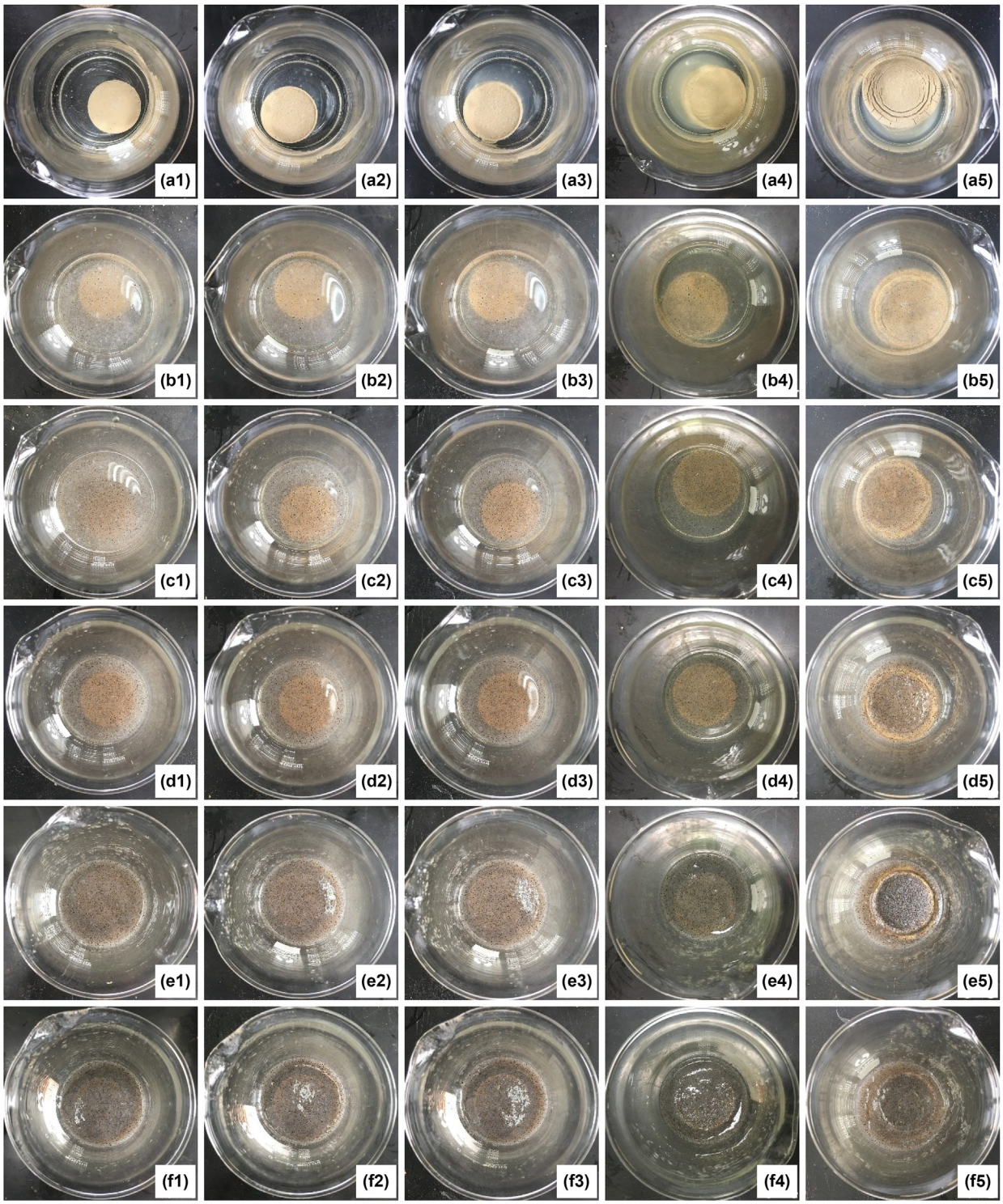

Fig. 20. The variation of shale with time after immersing in different suspensions: (**a**) control sample; (**b**) 0.1 w/v% basil seed; (**c**) 0.3 w/v% basil seed; (**d**) 0.5 w/v% basil seed; (**e**) 1.0 w/v% basil seed; (**f**) 3.0 w/v% basil seed. Note: 1: 0 min; 2: 30 min; 3: 1 h; 4: 4 h; 5: 24 h.

properties in terms of rheology, filtration, shale hydration inhibition and lubrication. Except multifunctional, BSP also shows high environmental acceptability due to its biodegradability and non-toxicity. According to our statistics, the basil seeds have a low costs ranging from 8 to 11 thousands CNY (Chinese Yuan) per ton, while the price of generally used biopolymer of xanthan gum and guar gum is 13–15 and 8–13 thousand CNY per ton, respectively. In addition, BSPs can be obtained by simple grinding of basil seed without further treatment, whereas for xanthan gum, the preparation procedure includes several steps like bacterial seed screening and cultivation, fermentation and extraction (Habibi and Khosravi-Darani, 2017). In the case of guar gum, there are several steps including splitting, thermal dehusking, milling, dissolution, filtration, drying (Sharma et al., 2018). From the above analysis, BSP

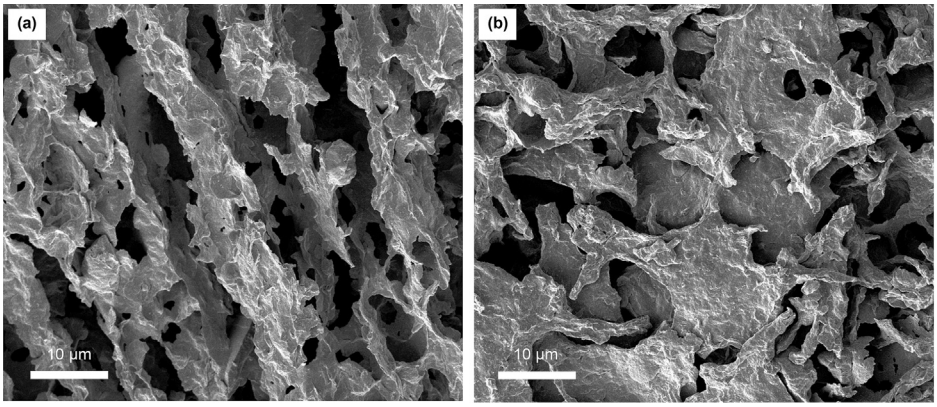

Fig. 21. SEM images of shale cores soaked at (**a**) deionized water and (**b**) 1.0 w/v% BSP suspension for 24 h.

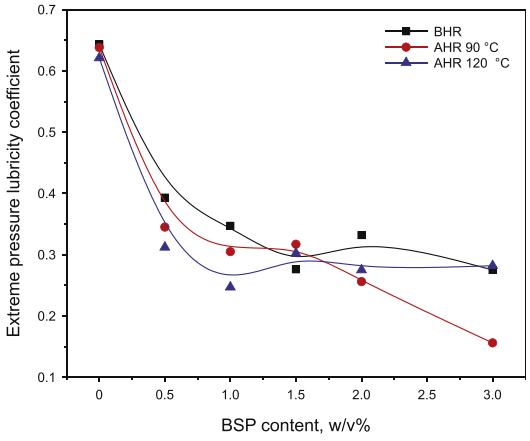

Fig. 22. Effect of basil seed on the lubrication properties of bentonite suspension.

shows promise as a cost effective, environmentally friendly and multifunctional additive in drilling fluid.

4. Conclusions

In this research, the possibility of using BSPs to improve the properties of water-based drilling fluids is explored. Based on the undertaken research, the following conclusions can be drawn.

(1) All the rheological studies between bentonite-BSP systems presents a shear thinning behavior. At low BSP concentrations the Bingham model fits the rheological data well, while at higher concentrations the power law model describes better, suggesting the rheological properties are predominately controlled by BSPs at high concentration. The bentonite suspension with BSPs can resist high temperature of 120 °C.

Table 7
The formulas of water-based drilling fluids for compatibility test.

Formula 1			Formula 2		
Additive	Function	Content	Additive	Function	Content
Water	Dispersed medium	400 mL	Water	Dispersed medium	400 mL
Sodium bentonite	Viscosifying and filtration control	16 g	Sodium bentonite	Viscosifying and filtration control	16 g
Polyanionic cellulose with low viscosity	Filtration reducer	2 g	Sulfonated phenolic resin	Filtration reducer	12 g
			Sulfonated lignite resin	Filtration reducer	12 g
Polyamine	Shale inhibitor	2 g	Amphoteric polymer	Encapsulator	0.4 g
KCl	Shale inhibitor	12 g	KCl	Shale inhibitor	12 g
Vegetable oil derivative	Lubricant	12 g	Vegetable oil derivative	Lubricant	12 g
Barite	Weighting material	100 g	Barite		100 g

Table 8
The effect of BSP on the rheological and filtration properties.

Testing sample	Testing condition	AV, mPa s	PV, mPa s	YP, Pa	YP/PV, Pa/(mPa s)	Gel strength, Pa		LTLP filtration, mL
						10 s	10 min	
Formula 1	BHR	21	16.5	4.5	0.27	0.25	0.25	7.6
	AHR	24	18	5.5	0.30	1.75	1.75	9.8
Formula 1 + 4 g BSP	BHR	28.5	21	7.5	0.36	2.75	6.50	6.4
	AHR	32.5	22	10.5	0.48	4.75	5.00	6.2
Formula 2	BHR	28.5	17	11.5	0.67	3.00	7.00	6.0
	AHR	21.5	17.5	4.0	0.23	1.50	4.00	6.8
Formula 2 + 4 g BSP	BHR	36.5	21	15.5	0.73	5.00	9.50	5.4
	AHR	32	23	9	0.39	2.50	5.00	4.2

(2) The BSPs are capable of reducing filtration alone and better than bentonite particles. BSPs have substantial effects on the reduction of filtration loss after thermal aging at 120 °C, but less efficiency after thermal aging at 150 °C due to thermal degradation. The filtration loss reduction rate of LTLP and HTHP filtration is 61% and 58% in the presence of 1.5 w/v% BSP, respectively, compared to control sample. Meanwhile, the incorporation of BSPs dramatically enhances the resistance of inorganic salts contamination of bentonite suspension. The base mud containing 1.0 w/v% BSP can resist 5.0 w/v% NaCl and 0.3 w/v% $CaCl_2$ contamination respectively.

(3) In terms of shale hydration and dispersion inhibition, BSPs exhibits superior properties to XC and KCl in inhibiting shale dispersion, comparable to PHPA. Meanwhile, a synergistic effect is observed when BSP and KCl are used in combination.

(4) BSP can reduce the friction and improve the lubricity effectively. About 60% lubricity coefficient reduction is observed after the addition of 1.0 w/v% BSP. The excellent water holding capacity and strong adsorption to form the hydration layers contribute to this low friction.

(5) The unique nanoscale 3D networks of BSP, as well as insoluble particles endow BSPs exceptional water retention ability and thickening effect. The interaction between the multiple groups of BSP and bentonite particles and metal surface results in the formation of hydration layer, which favors the filtration control, less shale hydration and dispersion, and low friction. The impressive properties delivered by BSP indicate that BSP is a multi-functional additive. In addition, the characteristics of renewable, non-toxic, and potentially less expensive show BSP has promise to replace conventional synthetic polymers.

Acknowledgements

This work was financially supported by CNPC Innovation Foundation (2020D-5007-0310), National Natural Science Foundation of China (No. 51974354) and National Key Research and Development Project (2019YFA0708303).

References

Ahmad, H.M., Kamal, M.S., Murtaza, M., Al-Harthi, M.A., 2017. Improving the drilling fluid properties using nanoparticles and water-soluble polymers. In: SPE Kingdom of Saudi Arabia Annual Technical Symposium and Exhibition, Dammam, 24-27 April. https://doi.org/10.2118/188140-MS.

Ahmad, H.M., Kamal, M.S., Al-Harthi, M.A., 2018. Rheological and filtration properties of clay-polymer systems: impact of polymer structure. Appl. Clay Sci. 160, 226–237. https://doi.org/10.1016/j.clay.2018.01.016.

Ahmed, H., Glass, J.E., McCarthy, G.J., 1981. Adsorption of water-soluble polymers on high surface area clays. In: 56th Annual Fall Technical Conference and Exhibition of the Society of Petroleum Engineers of AIME, Texas, 5-7 October. https://doi.org/10.2118/10101-MS.

Akbari, I., Ghoreishi, S.M., 2017. Generation of porous structure from basil seed mucilage via supercritical fluid assisted process for biomedical applications. Pharm Sci Dev Res 3 (1), 30–35. https://doi.org/10.17352/ijpsdr.000014.

Al-Hameedi, A.T., Alkinani, H.H., Dunn-Norman, S., Alashwak, N.A., Alshammari, A.F., Alkhamis, M.M., Albazzaz, H.W., Mutar, R.A., Alsaba, M.T., 2019a. Environmentally friendly drilling fluid additives: can food waste products be used as thinners and fluid loss control agents for drilling fluid?. In: SPE Symposium: Asia Pacific Health, Safety, Security, Environment and Social Responsibility, Malaysia, 23-24 April https://doi.org/10.2118/195410-MS.

Al-Hameedi, A.T., Alkinani, H.H., Dunn-Norman, S., Alshammari, A.F., Mutar, R., 2019b. A laboratory study of environmentally friendly drilling fluid additive to be exploited as a multifunctional bio-enhancer additive in water-based drilling fluid. In: AADE Fluids Technical Conference and Exhibition, Denver, 9-10 April. AADE-19-NTCE-SPP-01.

Barry, M.M., Jung, Y., Lee, J.-K., Phuoc, T.X., Chyu, M.K., 2015. Fluid filtration and rheological properties of nanoparticle additive and intercalated clay hybrid bentonite drilling fluids. J. Petrol. Sci. Eng. 127, 338–346. https://doi.org/10.1016/j.petrol.2015.01.012.

Benchabane, A., Bekkour, K., 2006. Effects of anionic additives on the rheological behavior of aqueous calcium montmorillonite suspensions. Rheol. Acta 45, 425–434. https://doi.org/10.1007/s00397-005-0063-1.

Browning, W.C., Perricone, A.C., 1963. Clay chemistry and drilling fluids. In: Drilling and Rock Mechanics Symposium, Texas, 23-24 January. https://doi.org/10.2118/540-MS.

Burchill, S., Hall, P.L., Harrison, R., Hayes, M.H.B., 1983. Smectite-polymer interactions in aqueous systems. Clay Miner. 18 (4), 373–397. https://doi.org/10.1180/claymin.1983.018.4.04.

Caenn, R., Chillingar, G.V., 1996. Drilling fluids: state of the art. J. Petrol. Sci. Eng. 14 (3–4), 221–230. https://doi.org/10.1016/0920-4105(95)00051-8.

Clements, W.R., Jarrett, M.A., Morton, E.K., 1987. A new class of filtration control polymers offers exceptional electrolyte tolerance. In: SPE Annual Technical Conference and Exhibition, Texas, 27-30 September. https://doi.org/10.2118/16686-MS.

Davoodi, S., Ramazani, S.A.A., Jamshidi, S., Jahromi, A.F., 2018. A novel field applicable mud formula with enhanced fluid loss properties in high pressure-high temperature well condition containing pistachio shell powder. J. Petrol. Sci. Eng. 162, 378–385. https://doi.org/10.1016/j.petrol.2017.12.059.

De Oliveira, V.A.V., Alves, K.D.S., Silva-Junior, A.A.D., Araújo, R.M., Balaban, R.C., Hilliou, L., 2020. Testing carrageenans with different chemical structures for water-based drilling fluid application. J. Mol. Liq. 299, 1–9. https://doi.org/10.1016/j.molliq.2019.112139.

Dhanke, P., Wagh, S., 2020. Treatment of vegetable oil refinery wastewater with biodegradability index improvement. Mater Today Proc 27, 181–187. https://doi.org/10.1016/j.matpr.2019.10.004.

Dong, X., Wang, L., Yang, X., Lin, Y., Xue, Y., 2015. Effect of ester based lubricant SMJH-1 on the lubricity properties of water based drilling fluid. J. Petrol. Sci. Eng. 135, 161–167. https://doi.org/10.1016/j.petrol.2015.09.004.

Farahmandfar, R., Naji-Tabasi, S., 2020. Influence of different salts on rheological and functional properties of basil (Ocimum bacilicum L.) seed gum. Int. J. Biol. Macromol. 149, 101–107. https://doi.org/10.1016/j.ijbiomac.2020.01.170.

Ghaderi, S., Haddadi, S.A., Davoodi, S., Arjmand, M., 2020. Application of sustainable saffron purple petals as an eco-friendly green additive for drilling fluids: a rheological, filtration, morphological, and corrosion inhibition study. J. Mol. Liq. 315, 1–17. https://doi.org/10.1016/j.molliq.2020.113707.

Ghaleh, S.P., Khodapanah, E., Tabatabaei-Nezhad, S.A., 2020. Experimental evaluation of thiamine as a new clay swelling inhibitor. Petrol. Sci. 17 (6), 1616–1633. https://doi.org/10.1007/s12182-020-00466-6.

Guerrero, M., Guerrero, X., 2006. Use of amine/PHPA system to drill high reactive shales in the Orito field in Colombia. In: International Oil Conference and Exhibition in Mexico, Cancun, 31 August-2 September. https://doi.org/10.2118/104010-MS.

Gudarzifar, H., Sabbaghi, S., Rezvani, A., Saboori, R., 2020. Experimental investigation of rheological & filtration properties and thermal conductivity of water-based drilling fluid enhanced. Powder Technol. 368, 323–341. https://doi.org/10.1016/j.powtec.2020.04.049.

Guo, Q., Cui, S.W., Wang, Q., Goff, H.D., Smith, A., 2009. Microstructure and rheological properties of psyllium polysaccharide gel. Food Hydrocolloids 23 (6), 1542–1547. https://doi.org/10.1016/j.foodhyd.2008.10.012.

Habibi, H., Khosravi-Darani, K., 2017. Effective variables on production and structure of xanthan gum and its food applications: a review. Biocatal. Agr. Biotechnol. 10, 130–140. https://doi.org/10.1016/j.bcab.2017.02.013.

Hall, L.J., Deville, J.P., Araujo, C.S., Li, S., Rojas, O.J., 2017. Nanocellulose and its derivatives for high-performance water-based fluids. In: SPE International Conference on Oilfield Chemistry, Texas, 3–5 April. https://doi.org/10.2118/184576-MS.

Hall, L.J., Deville, J.P., Santos, C.M., Rojas, O.J., Araujo, C.S., 2018. Nanocellulose and biopolymer blends for high-performance water-based drilling fluids. In: SPE-189577-MS, IADC/SPE Drilling Conference and Exhibition, Texas, 6-8 March. https://doi.org/10.2118/189577-MS.

Hiller, K.H., 1963. Rheological measurements on clay suspensions and drilling fluids at high temperatures and pressures. J. Petrol. Technol. 15 (7), 779–789. https://doi.org/10.2118/489-PA.

Hossain, M.E., Wajheeuddin, M., 2016. The use of grass as an environmentally friendly additive in water-based drilling fluids. Petrol. Sci. 13, 292–303. https://doi.org/10.1007/s12182-016-0083-8.

Hosseini-Parvar, S.H., Matia-Merino, L., Goh, K.K.T., Razavi, S.M.A., Mortazavi, S.A., 2010. Steady shear flow behavior of gum extracted from Ocimum basilicum L. seed: effect of concentration and temperature. J. Food Eng. 101, 236–243. https://doi.org/10.1016/j.jfoodeng.2010.06.025.

Johannes, K.F., 2012. Petroleum Engineer's Guide to Oil Field Chemicals and Fluids. Gulf Professional Publishing, Waltham, USA.

Kafashi, S., Rasaei, M., Karimi, G., 2017. Effects of sugarcane and polyanionic cellulose on rheological properties of drilling mud: an experimental approach. Egypt J Petrol 26, 371–374. https://doi.org/10.1016/j.ejpe.2016.05.009.

Kelessidis, V.C., Zogtafou, M., Chatzistamou, V., 2013. Optimization of drilling fluid rheological and fluid loss properties utilizing PHPA polymer. In: SPE Middle East Oil and Gas Show and Conference, Bahrain, 10-13 March. https://doi.org/10.2118/164351-MS.

Kumar, S., Thakur, A., Kumar, N., Husein, M.M., 2020. A novel oil-in-water drilling mud formulated with extracts from Indian mango seed oil. Petrol. Sci. 17 (1), 196–210. https://doi.org/10.1007/s12182-019-00371-7.

Kuppusamy, S., Jayaraman, N., Jagannathan, M., Kadarkarai, M., Aruliah, R., 2017. Electrochemical decolorization and biodegradation of tannery effluent for reduction of chemical oxygen demand and hexavalent chromium. J Water Proces Eng 20, 22–28.

Leerlooijer, K., Kuijvenhoven, C.A.T., Francis, P.A., 1996. Filtration control, mud design and well productivity. In: SPE Formation Damage Control Symposium, Lafayette, LA, 14–15 February. https://doi.org/10.2118/31079-MS.

Li, J., Liu, Y., Luo, J., Liu, P., Zhang, C., 2012. Excellent lubricating behavior of Brasenia schreberi mucilage. Langmuir 28, 7797–7802. https://doi.org/10.1021/la300957v.

Li, M.-C., Ren, S., Zhang, X., Dong, L., Lei, T., Lee, S., Wu, Q., 2018. Surface-chemistry-tuned cellulose nanocrystals in a bentonite suspension for water-based drilling fluids. ACS Appl Nano Mater 1 (12), 7039–7051. https://doi.org/10.1021/acsanm.8b01830.

Li, M.C., Wu, Q., Song, K., Lee, S., Jin, C., Ren, S., Lei, T., 2015. Soy protein isolate as fluid loss additive in bentonite-water-based drilling fluids. ACS Appl. Mater. Interfaces 7, 24799–24809. https://doi.org/10.1021/acsami.5b07883.

Li, W., Zhao, X., Li, Y., Ji, Y., Peng, H., Liu, L., Yang, Q., 2015. Laboratory investigations on the effects of surfactants on rate of penetration in rotary diamond drilling. J. Petrol. Sci. Eng. 134, 114–122. https://doi.org/10.1016/j.petrol.2015.07.027.

Li, W., Zhao, X., Ji, Y., Peng, H., Li, Y., Liu, L., Han, X., 2016. An investigation on environmentally friendly biodiesel-based invert emulsion drilling fluid. J Pet Explor Prod Technol 6 (3), 505–517. https://doi.org/10.1007/s13202-015-0205-7.

Li, W., Zhao, X., Ji, Y., Peng, H., Chen, B., Liu, L., Han, X., 2016. Investigation of biodiesel-based drilling fluid, Part 1: biodiesel evaluation, invert-emulsion properties, and development of a novel emulsifier package. SPE J. 21 (5), 1755–1766. https://doi.org/10.2118/180918-PA.

Li, W., Zhao, X., Ji, Y., Peng, H., Chen, B., Liu, L., Han, X., 2016. Investigation of biodiesel-based drilling fluid, part 2: formulation design, rheological study, and laboratory evaluation. SPE J. 21 (5), 1767–1781. https://doi.org/10.2118/180926-PA.

Li, W., Zhao, X.H., Peng, H., Guo, J., Ji, T., Chen, B., You, Z., Liu, L., 2016. A novel environmentally friendly lubricant for water-based drilling fluids as a new application of biodiesel. In: IADC/SPE Asia Pacific Drilling Technology Conference, Singapore, 22–24 August. https://doi.org/10.2118/180565-MS.

Li, W., Liu, J., Zhao, X., Zhang, J., Jiang, J., He, T., Liu, L., Shen, P., Zhang, M., 2018. Novel modified rectorite provides reliable rheology and suspendability for biodiesel based drilling fluid. In: SPE/IADC Middle East Drilling Technology Conference and Exhibition. UAE, Abu Dhabi. https://doi.org/10.2118/189310-MS, 29-31 January.

Li, W., Liu, J., Zhao, X., Jiang, J., Peng, H., Zhang, M., He, T., Liu, G., Shen, P., 2019. Development and screening of additives for biodiesel based drilling fluids: principles, strategies and experience. In: SPE International Conference on Oilfield Chemistry, Galveston, Texas, USA, 8-9 April. https://doi.org/10.2118/193597-MS.

Liu, P., Liu, Y., Yang, Y., Chen, Z., Li, J., Luo, J., 2014. Mechanism of biological liquid superlubricity of brasenia schreberi mucilage. Langmuir 30 (13), 3811–3816. https://doi.org/10.1021/la500193n.

Lodhi, B.A., Hussain, M.A., Sher, M., Haseeb, M.T., Ashraf, M.U., Hussain, S.Z., Hussain, I., Bukhari, S.N.A., 2019. Polysaccharide-based superporous, superabsorbent, and stimuli responsive hydrogel from sweet basil: a novel material for sustained drug release. Adv. Polym. Technol. 1–11. https://doi.org/10.1155/2019/9583516, 2019.

Luckham, P.F., Rossi, S., 1999. The colloidal and rheological properties of bentonite suspensions. Adv. Colloid Interface Sci. 82, 43–92. https://doi.org/10.1016/S0001-8686(99)00005-6.

Luo, Z., Wang, L., Pei, J., Yu, P., Xia, B., 2018. A novel star-shaped copolymer as a rheology modifier in water-based drilling fluids. J. Petrol. Sci. Eng. 168, 98–106. https://doi.org/10.1016/j.petrol.2018.05.003.

Milner, P.E., Parkes, M., Puetzer, J.L., Chapman, R., Stevens, M.M., Cann, P., Jeffers, J.R.T., 2018. A low friction, biphasic and boundary lubricating hydrogel for cartilage replacement. Acta Biomater. 65, 111. https://doi.org/10.1016/j.actbio.2017.11.002, 02.

Mirabolhassani, S.E., Rafe, A., Razavi, S.M.A., 2016. The influence of temperature, sucrose and lactose on dilute solution properties of basil (Ocimumbasilicum) seed gum. Int. J. Biol. Macromol. 93, 623–629. https://doi.org/10.1016/j.ijbiomac.2016.09.021.

Moslemizadeh, A., Shadizadeh, S.R., Moomenie, M., 2015. Experimental investigation of the effect of henna extract on the swelling of sodium bentonite in aqueous solution. Appl. Clay Sci. 105–106, 78–88. https://doi.org/10.1016/j.clay.2014.12.025.

Naji-Tabasi, S., Razavi, S.M.A., Mohebbi, M., Malaekeh-Nikouei, B., 2016. New studies on basil (Ocimum bacilicum L) seed gum part I-fractionation, physicochemical and surface activity characterization. Food Hydrocolloids 52, 350–358. https://doi.org/10.1016/j.foodhyd.2015.07.011.

Naji-Tabasi, S., Razavi, S.M.A., 2017. Functional properties and applications of basil seed gum: an overview. Food Hydrocolloids 73, 313–325. https://doi.org/10.1016/j.foodhyd.2017.07.007.

Naji-Tabasi, S., Razavi, S.M.A., 2017. New studies on basil (ocimum bacilicum L.) seed gum part III- steady and dynamic shear rheology. Food Hydrocolloids 67, 243–250. https://doi.org/10.1016/j.foodhyd.2015.12.020.

Nazir, S., Wani, I.A., Masoodi, F.A., 2017. Extraction optimization of mucilage from basil (Ocimum basilicum L.) seeds using response surface methodology. J. Adv. Res. 8 (3), 235–244. https://doi.org/10.1016/j.jare.2017.01.003.

Nicora, L.F., McGregor, W.M., 1998. Biodegradable surfactants for cosmetics find application in drilling fluids. In: IADC/SPE Drilling Conference, Texas, 3-6 March. https://doi.org/10.2118/39375-MS.

Ogugbue, C.E., Rathan, M.P., Shah, S.N., 2010. Experimental investigation of biopolymer and surfactant based fluid blends as reservoir drill-in fluids. In: SPE Oil and Gas India Conference and Exhibition, Mumbai, 20–22 January. https://doi.org/10.2118/128839-MS.

Okon, A.N., Ju, Akpabio, Tugwell, K.W., 2020. Evaluation the locally sourced materials as fluid loss control additives in water-based drilling fluid. Heliyon 6. https://doi.org/10.1016/j.heliyon.2020.e04091, 1-16.

Otieno, B., Apollo, S., Kabuba, J., Naidoo, B., Simate, G., Ochieng, A., 2019. Ozonolysis pre-treatment of waste activated sludge for solubilization and biodegradability enhancement. J Environ Chem Eng 7, 102945. https://doi.org/10.1016/j.jece.2019.102945.

Plank, J.P., Gossen, F.A., 1991. Visualization of fluid-loss polymers in drilling-mud filter cakes. SPE Drill. Eng. 6 (3), 203–208. https://doi.org/10.2118/19534-PA.

Rafe, A., Razavi, M.A., Farhoosh, R., 2013. Rheology and microstructure of basil seed gum and β-lactoglobulin mixed gels. Food Hydrocolloids 30 (1), 134–142. https://doi.org/10.1016/j.foodhyd.2012.05.016.

Rafe, A., Razavi, S.M.A., 2013. Dynamic viscoelastic study on the gelation of basil seed gum. Int. J. Food Sci. Technol. 48, 556–563. https://doi.org/10.1111/j.1365-2621.2012.03221.x.

Salmachi, A., Talemi, P., Tooski, Z.Y., 2016. Psyllium husk in water-based drilling fluids: an environmentally friendly viscosity and filtration agent. In: Abu Dhabi International Petroleum Exhibition & Conference, Abu Dhabi, 7–10 November. https://doi.org/10.2118/183308-MS.

Samateh, M., Pottachal, N., Manafirasi, S., Vidysagar, A., Maldarelli, C., John, G., 2018. Unravelling the secret of seed-based gels in water: the nanoscale 3D network formation. Sci. Rep. 8, 1–8. https://doi.org/10.1038/s41598-018-25691-3.

Sarber, J.G., Reynolds, C., Michel, C.M., Haag, K., Morris, R.A., 2010. The use of diutan biopolymer in coiled tubing drilling mud systems on the North Slope of Alaska. In: SPE/ICo TA Coiled Tubing and Well Intervention Conference and Exhibition, Texas, 23–24 March. https://doi.org/10.2118/130584-MS.

Shah, S., Heinle, S.A., Glass, J.E., 1985. Water-soluble polymer adsorption from saline solutions. In: SPE Oilfield and Geothermal Chemistry Symposium, Arizona, 9-11 March. https://doi.org/10.2118/13561-MS.

Sharma, G., Sharma, S., Kumar, A., Al-Muhtaseb, A.H., Naushad, M., Ghfar, A.A., Mola, G.T., Stadler, F.J., 2018. Guar gum and its composites as potential materials for diverse applications: a review. Carbohydr. Polym. 199, 534–545. https://doi.org/10.1016/j.carbpol.2018.07.053.

Tehrani, M.A., Popplestone, A., Guarneri, A., Carminati, S., 2007. Water-based drilling fluid for HT/HP applications. In: International Symposium on Oilfield Chemistry, Texas, 28 February-2 March. https://doi.org/10.2118/105485-MS.

Tomiwa, Q., Oluwatosin, R., Temiloluwa, O., Oluwasanmi, O., Joy, I., 2019. Improved water based mud using solanum tuberosum formulated biopolymer and application of artificial neural network in predicting mud rheological properties. In: SPE 198861, Nigeria Annual International Conference and Exhibition, Lagos, 5-7 August. https://doi.org/10.2118/198861-MS.

Vargas, J., Roldán, L.J., Lopera, S.H., Cardenas, J.C., Zabala, R.D., Franco, C.A., Cortés, F.B., 2019. Effect of silica nanoparticles on thermal stability in bentonite free water-based drilling fluids to improve its rheological and filtration properties after aging process. In: Offshore Technology Conference Brasil, Rio de Janeiro, 29–31 October. https://doi.org/10.4043/29901-MS.

Villada, Y., Gallardo, F., Erdmann, E., Casis, N., Olivares, L., Estenoz, D., 2017. Functional characterization on colloidal suspensions containing xanthan gum (XGD) and polyanionic cellulose (PAC) used in drilling fluids for a shale formation. Appl. Clay Sci. 149, 59–66. https://doi.org/10.1016/j.clay.2017.08.020.

Xu, Z., Sun, Y., Niu, Z., Xu, Y., Wei, X., Chen, X., Pan, D., Wu, W., 2020. Kinetic determination of sedimentation for GMZ bentonite colloids in aqueous solution: effect of pH, temperature and electrolyte concentration. Appl. Clay Sci. 184, 105393 https://doi.org/10.1016/j.clay.2019.105393.

Zameni, A., Kashaninejad, M., Aalami, M., Salehi, F., 2015. Effect of thermal and freezing treatments on rheological, textural and color properties of basil seed gum. J. Food Sci. Technol. 52 (9), 5914–5921. https://doi.org/10.1007/s13197-014-1679-x.

Zhang, L., Liu, Y., Chen, Z., Liu, P., 2016. Behavior and mechanism of ultralow friction of basil seed gel. Colloid. Surface. 489, 454–460. https://doi.org/10.1016/j.colsurfa.2015.11.019.

Zhang, X., Dong, L., Lei, T., Lee, S., Wu, Q., 2018. Surface-chemistry-tuned cellulose nanocrystals in a bentonite suspension for water-based drilling fluids. ACS Appl Nano Mater 1, 7039–7051. https://doi.org/10.1021/acsanm.8b01830.

Zhong, H., Shen, G., Qiu, Z., Lin, Y., Fan, L., Xing, X., Li, J., 2019. Minimizing the HTHP filtration loss of oil-based drilling fluid with swellable polymer microspheres. J. Petrol. Sci. Eng. 172, 411–424. https://doi.org/10.1016/j.petrol.2018.09.074.